Inorganic Chemistry
ARTICLE
pubs.acs.org/IC

From Simple to Complex: Topological Evolution and Luminescence Variation in a Copper(I) Pyridylpyrazolate System Tuned via Second Ligating Spacers

Shun-Ze Zhan, Mian Li, Xiao-Ping Zhou, Jia Ni, Xiao-Chun Huang, and Dan Li*

Department of Chemistry, Shantou University, Guangdong 515063, People's Republic of China

S *Supporting Information*

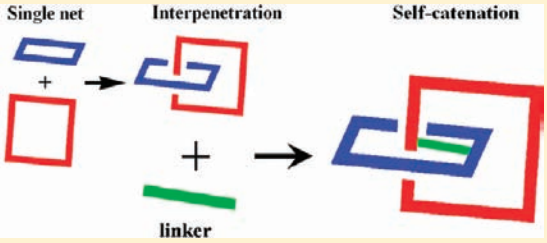

ABSTRACT: By systematically varying the geometric length and electronic properties of the second ligating ligands of halogen (Cl$^-$, Br$^-$, and I$^-$) and pseudohalogen (CN$^-$, SCN$^-$, and N$_3$$^-$) anions, we synthesized 11 isomeric/isostructural copper(I) complexes: [Cu$_2$(**L3-3**)I]$_n$ (**1**), [Cu$_2$(**L4-4**)Br]$_n$ (**2-Br**), [Cu$_2$(**L4-4**)Cl]$_n$ (**2-Cl**), [Cu$_2$(**L3-4**)(CN)]$_n$ (**3**), [Cu$_2$(**L3-3**)(CN)]$_n$ (**4**), [Cu$_3$(**L4-4**)(CN)$_2$]$_n$ (**5**), {[Cu$_2$(**L4-4**)Br]$_2$·CuBr}$_n$ (**6-Br**), {[Cu$_2$(**L4-4**)Cl]$_2$·CuCl}$_n$ (**6-Cl**), [Cu$_2$(**L4-4**)(SCN)]$_n$ (**7α-SCN**), [Cu$_2$(**L4-4**)(SCN)]$_n$ (**7*β*-SCN**), and [Cu$_2$(**L4-4**)(N$_3$)]$_n$ (**7α-N$_3$**). These structures are based on a series of isomeric pyridylpyrazole ligands, namely, 3,5-bis(3-pyridyl)-1*H*-pyrazole (H**L3-3**), 3-(3-pyridyl)-5-(4-pyridyl)-1*H*-pyrazole (H**L3-4**), and 3,5-bis(4-pyridyl)-1*H*-pyrazole (H**L4-4**), and their structural features range from 1-D (**1**), 2-D (**2**), and 3-D noninterpenetration (**3**), to 3-D 2-fold interpenetration (**4** and **5**), to 3-D self-catenation (**6** and **7**), exhibiting a trend from simple to complex with dimension expansion and an interpenetrating degree increase. The five most complex structures (**6** and **7**) with self-catenated networks are based on 2-fold interpenetrated networks linked via appropriate second ligating spacers (Cl$^-$, Br$^-$, SCN$^-$, and N$_3$$^-$), representing a strategy to construct self-catenated coordination polymers through cross-linking interpenetrated frameworks. Moreover, these complexes exhibit strong photoluminescence, which is mainly ascribed to Cu^{I}-related charge transfers (MLCT, MC, and MMLCT) regulated by the electronic properties of halogen or pseudohalogen. The topological evolution and luminescence variation presented in this work open an avenue to understanding the luminescence origin and the structure–property relationship of luminescent coordination polymers.

■ INTRODUCTION

The design and synthesis of coordination polymers with special structures and properties are of great interest because of their widely potential applications in functional materials.[1−4] However, it is difficult to predict their exact structures because many factors may influence the resulting structures.[5,6] Entangled systems, including discrete and polymeric ones, are among the most complicated structures and have become a vital theme of supramolecular coordination chemistry, owing to their applications in molecular devices,[7] photochemical and photophysical properties[8] and gas adsorption,[3,4] as well as their aesthetic architectures and topologies.[9−12] In contrast to the conventional strategy of using long and exomultidentate ligands[9a,b,10a] to construct multi-interpenetrated networks, recently, a handful of new protocols, such as templating[13a] and the "liquid-phase epitaxy" method,[13b] have been applied to manipulate the catenation manner and interpenetration degree of entangled coordination polymers and thus improve their properties, such as density,[14] gas uptake,[6e,13a] and luminescence.[8b]

Among other entangled systems, the phenomenon of self-catenation (also known as self-penetration, self-entanglement, and polyknotting) is rare and unpredicted.[9,11,12] The term of *self-catenation* proposed by Proserpio et al.[15] describes a special single network in which the smallest topological rings are penetrated by the rods belonging to the same net.[9a−c,15] Recently, more and more self-catenated complexes have been reported,[9−12] but it is still a formidable task for chemists to synthesize self-catenated coordination polymers by judiciously selecting appropriate ligands and metals. Interestingly, a small number of self-catenated networks are built through the cross-linking of different types of interpenetrated networks connected by bridging ligands or supramolecular interactions.[9a,b,10b,10c,11a,11b,12] For example, Schröder et al. showed a typical 6-connected self-catenated network constructed from 5-fold interpenetrated diamond networks cross-linked via water molecules,[10b] and Lin et al. reported an even more interesting case of crystal transformation of 3-D 2-fold interpenetrated coordination polymers to self-catenated coordination polymers.[12] These prompt us to explore a general strategy of constructing self-catenated systems through the cross-linking of multifold interpenetrated frameworks via appropriate linear connectors, as shown in Scheme 1. In this work, we focus on extending our previous work on a pair of self-catenated isomers,[11a] based on our continuous investigation of the copper(I)

Received: April 23, 2011
Published: August 24, 2011

Scheme 1. Schematic Representation of the Formation of a Self-Catenated System Constructed from the Cross-Linking of Interpenetrated Frameworks via Linear Connectors

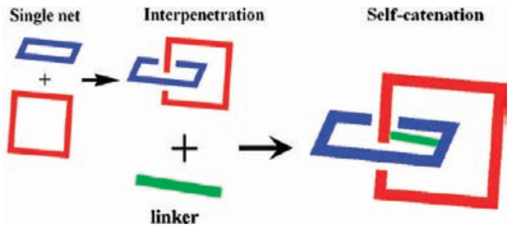

Chart 1. Illustration of the Ligands

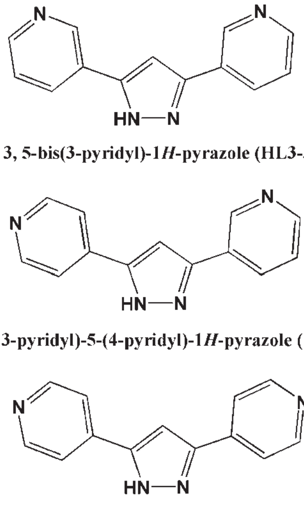

3, 5-bis(3-pyridyl)-1*H*-pyrazole (HL3-3)

3-(3-pyridyl)-5-(4-pyridyl)-1*H*-pyrazole (HL3-4)

3,5-bis(4-pyridyl)-1*H*-pyrazole (HL4-4)

pyridylpyrazolate system, and systematically examining the effect of the second ligating spacers of halogen (Cl^-, Br^-, and I^-) and pseudohalogen (CN^-, SCN^-, and $N_3{}^-$) anions.

On the other hand, such a systematic structural and topological investigation will facilitate research on the structure−property relationship of coordination materials, which aims at tuning the properties by tailoring the structures (including their electronic properties, steric effects, and space groups).[16−18] A rational strategy to explore the structure−property relationship is to design and synthesize a series of analogous materials such as isomers and isostructures. The work of Ford et al.[19] on the luminescence origin of $Cu_4X_4L_4$ (X = Cl^-, Br^-, and I^-; L = N- or P-based ligands) through investigation of a series of isostructures is a supreme example of studying the structure−property relationship of luminescent copper(I) clusters. In this work, the luminescence properties of the prepared copper(I) pyridylpyrazolate coordination polymers with closely related structures and topologies are measured and discussed.

Herein, we report our research on the synthesis, structure, and luminescence of a copper(I) pyridylpyrazolate system tuned via second ligating spacers. The 11 targeted coordination polymers are based on a series of isomeric, long-shaped, and multidentate ligands, namely, 3,5-bis(3-pyridyl)-1*H*-pyrazole (**HL3-3**),[20a,b] 3-(3-pyridyl)-5-(4-pyridyl)-1*H*-pyrazole (**HL3-4**), and 3,5-bis(4-pyridyl)-1*H*-pyrazole (**HL4-4**)[11a,20c] (Chart 1). These ligands all have side-armed *N*-pyridyl atoms (with distances ranging from 8 to 11 Å) to construct extended 2-D or 3-D networks, preferably with a certain degree of entanglement. The pyrazolate groups can act as 1,2-dihapto exobidentate ligands to bind two coinage metal ions, which may exhibit metal-based luminescence due to metal−metal interaction.[11a,20c,21−23] Halides (Cl^-, Br^-, and I^-) and pseudohalides (CN^-, SCN^-, and $N_3{}^-$) are selected as second ligating spacers and balance charges.[11a−d,19b,22b,23−26] With little steric hindrance, such kinds of small anions are perfect candidates as linear connectors to cross-link multifold interpenetrated frameworks.[11a] According to the literature,[11a,20c,24,27] the luminescence origin of this ternary system [copper(I), pyridylpyrazolate and halides/pseudohalides] can be tentatively assigned to various charge transfers related to the Cu^I center, such as metal-to-ligand charge transfer (MLCT), ligand-to-metal charge transfer (LMCT), halide/pseudohalide-to-metal charge transfer (XMCT), cluster-centered (CC) or metal-centered (MC), and even halide-to-ligand charge transfer (XLCT).[17,19] These will also be discussed along with the presented results.

■ EXPERIMENTAL SECTION

Materials and Physical Measurements. Commercially available chemicals were purchased and used without further purification. IR spectra were obtained in KBr disks on a Nicolet Avatar 360 FTIR spectrometer in the range of 4000−400 cm^{-1}. ^1H NMR spectroscopy measurements were performed on a Bruker DPX 400 spectrometer using tetramethylsilane as the internal standard. All chemical shift values (δ) are given in ppm. Elemental analyses of C, H, and N were determined with a Perkin-Elmer 2400C elemental analyzer. Thermogravimetric analyses (TGA) were performed on a Perkin-Elmer TGA7 instrument in flowing N_2 with a heating rate of 10 °C/min. Power X-ray diffraction (PXRD) experiments were performed on a D8 Advance X-ray diffractometer. Excitation and emission spectra were obtained on an Edinburg FLS920 spectrometer equipped with a continuous Xe900 xenon lamp. In all cases, purified single crystalline samples were used for the photoluminescence measurements.

Syntheses. *Ligands. 3,5-Bis(4-pyridyl)-1H-pyrazole (**HL4-4**) and 3,5-Bis(3-pyridyl)-1H-pyrazole (**HL3-3**).* The preparations were reported in our previous works.[11a,20a,c]

*3-(3-Pyridyl)-5-(4-pyridyl)-1H-pyrazole (**HL3-4**).* Step 1: 1-(3-Pyridyl)-3-(4-pyridyl)-l,3-propanedione. To a suspension of NaH (80% in oil, 1.5 g, 0.05 mol) in 50 mL of anhydrous tetrahydrofuran (THF) was added 3.5 mL (3.5 g, 0.025 mol) of methyl nicotinate. The mixture was stirred at room temperature for 10 min, and then 3.5 mL (3.5 g, 0.025 mol) of 4-acetylpyridine was slowly added to the mixture. After the addition of 4-acetylpyridine was completed, the mixture was allowed to stir for about 5 h. The mixture was filtered. A yellow solid was obtained and washed twice with 20 mL of THF and then dissolved in 50 mL of a diluted acetic acid solution (3 mol/L). The mixture was stirred for 30 min and then filtered. A yellow solid was obtained and dried in vacuum to give 4.3 g of the primary product, 1-(3-pyridyl)-3-(4-pyridyl)-l,3-propanedione. Yield: 63.9%. Mp: 198−200 °C. IR (ν/cm^{-1}): 3100 m, 3032 m, 2935 m, 1590 vs, 1540 vs, 1460 s, 1253 m, 1110 m, 1016 m, 796 s. ^1H NMR (400 MHz, $CDCl_3$, 298 K): δ 9.21 (d, *J* = 1.6 Hz, 1H, CHpy), 8.87 − 8.77 (m, 3H, CHpy), 8.29 (ddd, *J* = 8.4, 5.3, and 3.2 Hz, 1H, CHpy), 7.80 (dd, *J* = 4.5 and 1.7 Hz, 2H, CHpy), 7.48 (ddd, *J* = 8.0, 4.8, and 0.7 Hz, 1H, CHpy), 6.89 (s, 1H, C=CH).

Step 2: 3-(3-Pyridyl)-5-(4-pyridyl)-1*H*-pyrazole (**HL3-4**). A total of 2.3 g (0.01 mol) of 1-(3-pyridyl)-3-(4-pyridyl)-l,3-propanedione was added in ethanol (50 mL), and the mixture was treated with an excess of hydrazine (80%, 3 mL) and then refluxed for 10 h. The solution was allowed to stand in air to evaporate the ethanol solvent. Several days later colorless microcrystals were obtained to give 1.4 g of **HL3-4**. Yield: 62.5%. Mp: 230−232 °C. IR(ν/cm^{-1}): 3402 s, 3121 m, 3019 m, 1603 vs, 1425 s, 1221 m, 1000 m, 963 m, 824 s, 694 s. ^{1}H NMR (400 MHz, CD_3OD, 298 K): δ 8.99 (s, 1H, CHpy), 8.56 (d, J = 20.7 Hz, 3H, CHpy), 8.22 (d, J = 4.0 Hz, 1H, CHpy), 7.85 (d, J = 28.7 Hz, 2H, CHpy), 7.53 (s, 1H, CHpy), 7.35 (s, 1H, CHPz).

*Complexes. [Cu$_2$(**L3-3**)I]$_n$ (**1**).* A mixture of **HL3-3** (44.4 mg, 0.2 mmol), CuI (76.2 mg, 0.4 mmol), C_2H_5OH (10 mL), and aqueous NH_3 (0.5 mL) was sealed in a 15-mL Teflon-lined reactor, heated in an oven at 160 °C for 72 h, and slowly cooled to room temperature at a rate of 3 °C/30 min. Yellow block crystals were obtained (yield: 38% based on **HL3-3**). Anal. Calcd for $C_{13}H_9N_4ICu_2$: C, 32.86; H, 1.91; N, 11.79. Found: C, 32.65; H, 1.99; N, 11.49. IR data (KBr, cm^{-1}): 3109 m, 3056 w, 2921 w, 1610 s, 1569 m, 1467 vs, 1413 m, 1111 m, 997 m, 796 s, 698 s.

*[Cu$_2$(**L4-4**)Br]$_n$ (**2-Br**).* A mixture of **HL4-4**$\cdot 3H_2O$ (55.2 mg, 0.2 mmol), CuBr (57.6 mg, 0.4 mmol), C_2H_5OH (10 mL), and aqueous NH_3 (0.5 mL) was sealed in a 15-mL Teflon-lined reactor, heated in an oven at 140 °C for 72 h, and slowly cooled to room temperature at a rate of 3 °C/30 min. Light-yellow block crystals were obtained (yield: 45% based on **HL4-4**). Sometimes red block crystals could also be separated as complex **6-Br**. Anal. Calcd for $C_{13}H_9N_4BrCu_2$: C, 36.46; H, 2.12; N, 13.08. Found: C, 36.35; H, 1.97; N, 12.81. IR data (KBr, cm^{-1}): 3096 w, 3044 w, 2921 w, 1606 vs, 1466 s, 1421 m, 1209 m, 1102 m, 996 m, 804 s, 698 m.

*[Cu$_2$(**L4-4**)Cl]$_n$ (**2-Cl**).* A mixture of **HL4-4**$\cdot 3H_2O$ (55.2 mg, 0.2 mmol), $CuCl_2\cdot 2H_2O$ (68.4 mg, 0.4 mmol), C_2H_5OH (10 mL), and aqueous NH_3 (0.5 mL) was sealed in a 15-mL Teflon-lined reactor, heated in an oven at 140 °C for 72 h, and slowly cooled to room temperature at a rate of 3 °C/30 min. Light-yellow block crystals were obtained (yield: 38% based on **HL4-4**). Sometimes red block crystals could also be separated as complex **6-Cl**. Anal. Calcd for $C_{13}H_9N_4ClCu_2$: C, 40.68; H, 2.36; N, 14.60. Found: C, 40.42; H, 2.08; N, 14.35. IR data (KBr, cm^{-1}): 3056 w, 3021 w, 2930 w, 1604 vs, 1469 s, 1417 m, 1214 m, 1102 m, 998 m, 800 s, 698 m.

*[Cu$_2$(**L3-4**)(CN)]$_n$ (**3**).* Method 1: A mixture of **HL3-4** (44.4 mg, 0.2 mmol), $Cu(BF_4)_2\cdot 6H_2O$ (173 mg, 0.5 mmol), CH_3OH (10 mL), and aqueous NH_3 (0.5 mL) was sealed in a 15-mL Teflon-lined reactor, heated in an oven at 140 or 160 °C for 72 h, and slowly cooled to room temperature at a rate of 3 °C/30 min. Yellow block crystals were obtained (yield: 35% based on **HL3-4**). Note: The in situ formation of CN^- from methanol and aqueous NH_3 triggered by copper salt under solvothermal conditions was reported by us in ref 20c.

Method 2: A mixture of **HL3-4** (44.4 mg, 0.2 mmol), CuCN (36 mg, 0.4 mmol), C_2H_5OH (10 mL), and aqueous NH_3 (0.5 mL) was sealed in a 15-mL Teflon-lined reactor, heated in an oven at 140 or 160 °C for 72 h, and slowly cooled to room temperature at a rate of 3 °C/30 min. Yellow microcrystals were obtained (yield: 22% based on **HL3-4**). PXRD experiments showed that they were identical with those prepared from method 1. Anal. Calcd for $C_{14}H_9N_5Cu_2$: C, 44.92; H, 2.42; N, 18.71. Found: C, 44.71; H, 2.38; N, 18.52. IR data (KBr, cm^{-1}): 3068 w, 3011 w, 2112 vs, 1606 vs, 1466 m, 1225 m, 996 m, 833 s, 776 m, 694 m.

*[Cu$_2$(**L3-3**)(CN)]$_n$ (**4**).* A mixture of **HL3-3** (44.4 mg, 0.2 mmol), CuCN (36 mg, 0.4 mmol), CH_3OH (10 mL), and aqueous NH_3 (0.5 mL) was sealed in a 15-mL Teflon-lined reactor, heated in an oven at 160 °C for 72 h, and slowly cooled to room temperature at a rate of 3 °C/30 min. Near-colorless block crystals were obtained (yield: 35% based on **HL3-3**). Anal. Calcd for $C_{14}H_9N_5Cu_2$: C, 44.92; H, 2.42; N, 18.71. Found: C, 44.95; H, 2.46; N, 18.55. IR data (KBr, cm^{-1}): 3060 w, 3015 w, 2112 vs, 1601 vs, 1466 m, 1405 m, 1123 m, 996 m, 776 s, 694 s.

*[Cu$_3$(**L4-4**)(CN)$_2$]$_n$ (**5**).* A mixture of **HL4-4**$\cdot 3H_2O$ (55.2 mg, 0.2 mmol), CuCN (36 mg, 0.4 mmol), CH_3OH (10 mL), and aqueous NH_3 (0.5 mL) was sealed in a 15-mL Teflon-lined reactor, heated in an oven at 160 °C for 72 h, and slowly cooled to room temperature at a rate of 3 °C/30 min. Light-yellow block crystals were obtained (yield: 35% based on **HL4-4**). Anal. Calcd for $C_{15}H_9N_6Cu_3$: C, 38.84; H, 1.96; N, 18.12. Found: C, 38.54; H, 1.75; N, 18.00. IR data (KBr, cm^{-1}): 3117 w, 3060 w, 2128 vs, 1605 vs, 1470 m, 1217 m, 1172 m, 1004 m, 830 s, 771 m, 722 m.

*{[Cu$_2$(**L4-4**)Br]$_2$·CuBr}$_n$ (**6-Br**).* A mixture of **HL4-4**$\cdot 3H_2O$ (55.2 mg, 0.2 mmol), $CuBr_2$ (89.4 mg, 0.4 mmol), C_2H_5OH (10 mL), and aqueous NH_3 (0.5 mL) was sealed in a 15-mL Teflon-lined reactor, heated in an oven at 160 °C for 72 h, and slowly cooled to room temperature at a rate of 3 °C/30 min. Red block crystals were obtained (yield: 25% based on **HL4-4**). Anal. Calcd for $C_{26}H_{18}N_8Br_3Cu_5$: C, 31.23; H, 1.81; N, 11.21. Found: C, 31.15; H, 1.68; N, 11.15. IR data (KBr, cm^{-1}): 3117 w, 3051 w, 1609 vs, 1470 m, 1213 m, 1107 w, 1001 m, 845 s, 800 m, 727 m. Also complex **2-Br** could be separated as light-yellow microcrystals characterized by PXRD.

*{[Cu$_2$(**L4-4**)Cl]$_2$·CuCl}$_n$ (**6-Cl**).* A mixture of **HL4-4**$\cdot 3H_2O$ (55.2 mg, 0.2 mmol), $CuCl_2\cdot 2H_2O$ (68.4 mg, 0.4 mmol) C_2H_5OH (10 mL), and aqueous NH_3 (0.5 mL) was sealed in a 15-mL Teflon-lined reactor, heated in an oven at 160 °C for 72 h, and slowly cooled to room temperature at a rate of 3 °C/30 min. Red block crystals were obtained (yield: 41% based on **HL4-4**). Anal. Calcd for $C_{26}H_{18}N_8Cl_3Cu_5$: C, 36.04; H, 2.09; N, 12.93. Found: C, 36.10; H, 2.15; N, 12.81. IR data (KBr, cm^{-1}): 3109 w, 3043 w, 1605 vs, 1474 m, 1217 m, 1005 m, 837 m, 804 m, 730 m. Also complex **2-Cl** could be separated as light-yellow microcrystals characterized by PXRD.

*[Cu$_2$(**L4-4**)(SCN)]$_n$ (**7α-SCN**) and [Cu$_2$(**L4-4**)(SCN)]$_n$ (**7β-SCN**).* Refer to our previous communication.[11a]

*[Cu$_2$(**L4-4**)(N$_3$)]$_n$ (**7α-N$_3$**).* A mixture of **HL4-4**$\cdot 3H_2O$ (55.2 mg, 0.2 mmol), $Cu(BF_4)_2\cdot 6H_2O$ (173 mg, 0.5 mmol), NaN_3 (32.5 mg, 0.5 mmol), H_2O (10 mL), and aqueous NH_3 (0.5 mL) was sealed in a 15-mL Teflon-lined reactor, heated in an oven at 160 °C for 72 h, and slowly cooled to room temperature at a rate of 3 °C/30 min. Yellow column crystals were obtained (yield: 48% based on **HL4-4**). Anal. Calcd for $C_{13}H_9N_7Cu_2$: C, 40.00; H, 2.32; N, 25.12. Found: C, 39.92; H, 2.35; N, 25.05. IR data (KBr, cm^{-1}): 3097 w, 3026 w, 2055 vs, 2038 vs, 1605 vs, 1470 w, 1213 m, 1004 m, 833 m, 804 m.

Crystal Structure Determination. Suitable crystals were mounted with glue at the end of a glass fiber. Diffraction data were collected at 293(2) K with a Bruker-AXS SMART CCD area detector diffractometer using ω rotation scans with a scan width of 0.3 and Mo Kα radiation (λ = 0.710 73 Å). Multiscan absorptions were applied. The structure of **2-Cl** was solved by Patterson method and other structures were solved by direct method. All the structures were refined by full-matrix least-squares refinements based on F^2. The C/N atoms of CN^- in complexes **3**−**5** were undistinguishable and were refined with a 50% probability of being C or N and assigned randomly as C or N atoms. All non-H atoms were refined with anisotropic thermal parameters, and all H atoms were included in calculated positions and refined with isotropic thermal parameters riding on those of the parent atoms. Structure solutions and refinements were performed with the *SHELXL-97* package.[28] Crystal data and structure refinement details for these complexes are summarized in Table 1. Selected bond lengths and angles are given in Table S1 in the Supporting Information.

Structural and Topological Analysis. Structural and topological diagrams are exported through the computer programs of *OLEX*.[29] The point symbol and vertex symbol are computed using *TOPOS*.[30]

RESULTS AND DISCUSSION

Crystal Structures Description. *Complex **1**.* In complex **1**, each Cu^{I} atom is three-coordinated in a T-shaped geometry completed by one *N*-pyrazolate atom, one *N*-pyridyl atom, and one I atom (Figure 1a). The deprotonated **L3-3**, as a tetradentate ligand in a syn−syn conformation, is connected by Cu^{I} atoms nearly linearly through the N1B and N2 atoms [the N2−Cu1−N1B angle is 153.47(10)°], resulting in an infinite chain along the b axis

Table 1. Crystal Data and Structure Refinement Details for Complexes 1−7

parameter	1	2-Br	2-Cl	3	4
formula	$C_{13}H_9N_4Cu_2I$	$C_{13}H_9N_4Cu_2Br$	$C_{13}H_9N_4Cu_2Cl$	$C_{14}H_9N_5Cu_2$	$C_{14}H_9N_5Cu_2$
M_r	475.22	428.23	383.77	374.34	374.34
cryst syst	monoclinic	monoclinic	triclinic	monoclinic	tetragonal
space group	$P2_1/m$	$C2c$	$P\bar{1}$	$P2_1/n$	$I4_1/acd$
a (Å)	5.5325(7)	16.6627(19)	8.8528(18)	10.1968(9)	15.7482(9)
b (Å)	15.434(2)	9.7028(11)	9.3074(19)	8.8717(8)	15.7482(9)
c (Å)	7.7007(10)	10.1856(12)	9.786(2)	14.6262(14)	21.281(2)
α (deg)	90	90	62.417(3)	90	90
β (deg)	91.425(2)	125.461(2)	76.962(3)	90.062(2)	90
γ (deg)	90	90	66.016(3)	90	90
V (Å^3)	657.34(15)	1341.3(3)	652.3(2)	1323.1(2)	5277.8(7)
Z	2	4	2	4	16
D_{calcd} (g/cm^3)	2.401	2.121	1.954	1.879	1.884
μ (mm^{-1})	5.575	6.141	3.456	3.212	3.221
collected reflns	2563	4383	4598	7152	13573
unique reflns	1118	1593	2270	2338	1172
R_{int}	0.0125	0.0236	0.0158	0.0214	0.0335
R1^a [$I > 2\sigma(I)$]	0.0201	0.0574	0.0357	0.0279	0.0217
wR2^b [$I > 2\sigma(I)$]	0.0517	0.1794	0.0955	0.0714	0.0569
R1^a (all reflns)	0.0213	0.0641	0.0394	0.0309	0.0234
wR2^b (all reflns)	0.0525	0.1822	0.0982	0.0728	0.0577
GOF on F^2	1.072	1.275	1.093	1.059	1.057

parameter	5	6-Br	6-Cl	7α-N$_3$
formula	$C_{15}H_9N_6Cu_3$	$C_{26}H_{18}N_8Cu_5Br_3$	$C_{26}H_{18}N_8Cu_5Cl$	$C_{13}H_9N_7Cu_2$
M_r	463.90	999.91	866.53	390.35
cryst syst	monoclinic	monoclinic	monoclinic	orthorhombic
space group	$P2_1/n$	$C2/c$	$C2/c$	$Pbca$
a (Å)	5.6874(3)	15.1822(16)	15.2169(16)	11.398(3)
b (Å)	13.2637(7)	12.9042(14)	12.7604(14)	7.758(2)
c (Å)	20.5449(11)	14.4740(16)	14.1543(15)	29.507(8)
α (deg)	90	90	90	90
β (deg)	95.5100(10)	95.845(2)	95.614(2)	90
γ (deg)	90	90	90	90
V (Å^3)	1542.66(14)	2820.9(5)	2735.2(5)	2609.2(12)
Z	4	4	4	8
D_{calcd} (g/cm^3)	1.997	2.354	2.104	1.987
μ (mm^{-1})	4.106	7.993	4.153	3.266
collected reflns	8209	9674	9255	15284
unique reflns	2711	3459	3116	3126
R_{int}	0.0230	0.0281	0.0335	0.0403
R1^a [$I > 2\sigma(I)$]	0.0258	0.0271	0.0331	0.0937
wR2^b [$I > 2\sigma(I)$]	0.0643	0.0642	0.0792	0.1731
R1^a (all reflns)	0.0293	0.0349	0.0401	0.0983
wR2^b (all reflns)	0.0660	0.0665	0.0819	0.1788
GOF on F^2	1.046	1.059	1.095	1.400

^{a}R1 = $\Sigma(||F_o| - |F_c||)/\Sigma|F_o|$. ^{b}wR2 = $[\Sigma w(|F_o|^2| - |F_c|^2)^2/\Sigma w(F_o{}^2)^2]^{1/2}$.

(Figure 1c). Cu1 and its symmetry-related Cu1A are doubly bridged by the pyrazolate and I atoms in the usual mode of a μ_2 bridge, resulting in a familiar five-membered ring (I1−Cu1−N2−N2A−Cu1A). I atoms, hampered by the 3-pyridyl group, deviate severely from the Cu1−Cu1A−Pz plane, and the dihedral angle between the I1−Cu1−Cu1A and N2−N2A−Cu1A−Cu1 planes is about 50.2°. The distance of Cu1−Cu1A is 3.0565(8) Å, longer than 2.83 Å (the sum of the van der Waals radii).[31] These chains are piled together into the whole crystal through two different $\pi-\pi$ weak interactions between adjacent pyridyl rings, with center-to-center distances of 3.6376(2) Å (d_1) and 4.1371(3) Å (d_2) along the c axis, respectively (Figure 1b).

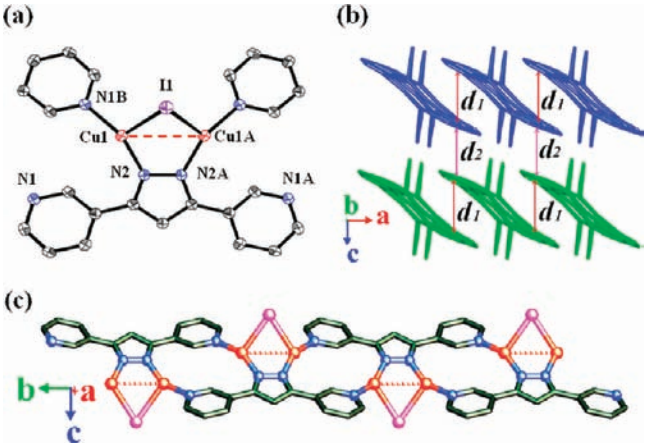

Figure 1. Structural diagrams of complex **1**: (a) ORTEP drawing of coordination environments with a 50% thermal ellipsoid; (b) packing diagram from the view along the *b* axis; (c) chain diagram. Symmetry codes: A, *x*, $-y + {}^{1}/_{2}$, *z*; B, $-x + 2$, $-y + 1$, $-z + 1$.

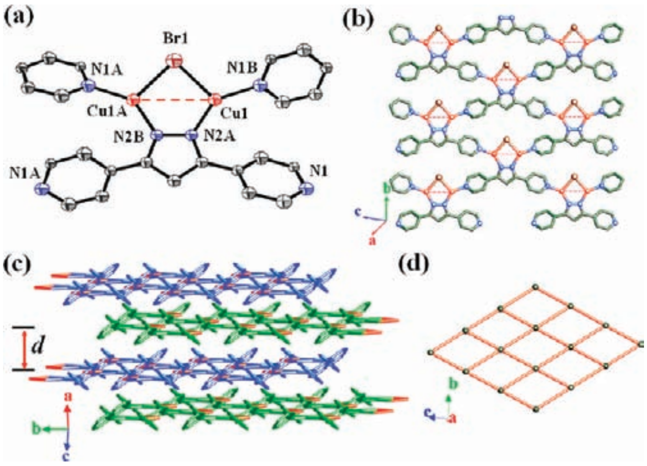

Figure 2. Structural diagrams of complex **2-Br**: (a) ORTEP drawing of coordination environments with a 50% thermal ellipsoid; (b) 2-D layer (one of the dangled pyridyl rings is omitted for clarity); (c) packing diagram showing the opposite directions of neighboring layers (Cu−Br bond: red); (d) (4,4) grid topology of a single layer. Symmetry codes: A, $-x + 1$, *y*, $-z + {}^{5}/_{2}$; B, $-x + {}^{1}/_{2}$, $y - {}^{1}/_{2}$, $-z + {}^{3}/_{2}$; C, $x + {}^{1}/_{2}$, $y - {}^{1}/_{2}$, $z + 1$.

Complex ***2-Br***. In complex **2-Br**, each Cu^{I} atom is three-coordinated in a T-shaped geometry completed by one *N*-pyrazolate atom, one *N*-pyridyl atom, and one Br atom (Figure 2a). Both the Br1 atom and pyrazolate doubly bridge symmetry-related Cu^{I} atoms (Cu1 and Cu1A) on one plane in a μ_2 mode, and the distance of the two Cu^{I} atoms is 3.2746(1) Å, much longer than 2.83 Å (the sum of the van der Waals radii).[31] Furthermore, the two Cu^{I} atoms are coordinated by *N*-pyridyl atoms from two other **L4-4** ligands, resulting in a 2-D sheet (Figure 2b) paralleling the [−1, 0, 2] crystallographic plane, in which almost all Cu^{I} atoms, Br atoms, and pyrazole rings are positioned on one plane, and the pyridyl rings are disordered along the C5−N1 bond [the dihedral angles between the disordered pyridyl ring and the plane of the 2-D layer are 37.66(2)° and 41.08(2)°]. These 2-D structures are piled alternately in opposite orientations (Br atoms of the two adjacent layers are positioned to opposite orientations) in the whole single crystal layer by layer (Figure 2c), and the distance between adjacent planes is equal [d = 4.008(1) Å]. It is clear that each sheet shows 2-D **sql** (4,4) topology[32] (Figure 2d).

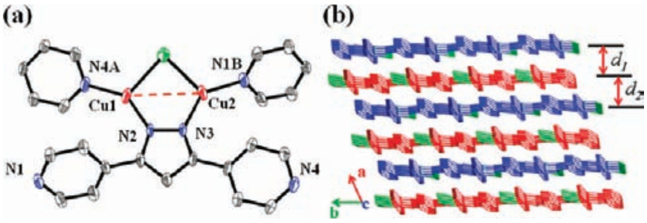

Figure 3. Structural diagrams of complex **2-Cl**: (a) ORTEP drawing of coordination environments with a 50% thermal ellipsoid; (b) packing diagram showing the opposite directions of neighboring layers (Cu−Cl bond: green) and *inter*layer distances. Symmetry codes: A, *x*, *y*, $z - 1$; B, *x*, $y - 1$, $z + 1$.

Complex ***2-Cl***. Complex **2-Cl** is very similar to complex **2-Br** in coordination environment and packing structure. However, it is crystallized in a triclinic system ($P\bar{1}$ space group), with lower symmetry than that of **2-Br**. The asymmetric unit contains one Cl atom, two Cu atoms (Cu1 and Cu2), and one whole **L4-4** ligand, in which two pyridyl rings are located at exact space positions (Figure 3a). The dihedral angles between the pyridyl and pyrazole rings are 26.49(5)° and 49.31(5)°, different from that of complex **2-Br**, and the Cl atoms are almost positioned on the Cu1−Cu2−pyrazole ring plane [the distance from Cl atoms to the plane is 0.089(7) Å]. The distance of the two Cu^{I} atoms bridged by pyrazole is 3.2312(2) Å, slightly shorter than that in **2-Br** and much longer than 2.83 Å (the sum of the van der Waals radii).[31] These 2-D sheets are piled layer by layer (Figure 3b) paralleling the [1, 0, 0] crystallographic plane, but the distances between these adjacent layers are slightly different [d_1 = 4.026(1) and d_2 = 4.052(1) Å], which may be related to its lower symmetry.

Complex ***3***. **3** is a 3-D polymer constructed from asymmetrical ligand **L3-4** and CuCN and contains two crystallographically independent Cu^{I} centers, one **L3-4** ligand, and one cyanide ligand (Figure 4a). As shown in Figure 4, the two Cu^{I} atoms are nearly coplanar with the pyrazolate ring bridging them, and the distance of the two Cu^{I} atoms is 3.0392(5) Å, longer than 2.83 Å (the sum of the van der Waals radii).[31] The two pyridyl groups are coordinated to two Cu^{I} atoms (3-pyridyl for Cu1 and 4-pyridyl for Cu2) from one side of the plane, and the other side is occupied by two cyanide ligands binding the two Cu^{I} atoms. As a whole, the tetradentate ligands **L3-4** are connected by Cu^{I} atoms to form a 2-D undulated layer structure (Figure 4b) with **sql** (4,4) grid topology parallel to the [1, 0, 1] plane. The layer contains two kinds of four-membered rings (Cu atoms as the corner of rings): one is formed by two whole **L3-4** ligands connecting two pairs of Cu^{I} atoms bridged by two pyrazolates from four *N*-pyridyl atoms (green shadow in Figure 4b); another is formed by four Cu^{I} atoms connected by four halves of **L3-4** ligands from one *N*-pyridyl atom and its close *N*-pyrazole atom of a **L3-4** ligand (red shadow in Figure 4b). Cyanide anions (green stick in Figure 4c) connect these parallel 2-D layers to form a 3-D structure with an unfamiliar uniform 5-connected topology (Figure 4d) with point symbol $\mathbf{4^{4}\cdot 6^{6}}$**-nov**,[33] in which two cyanide anions act as one linker to doubly bridge two $[Cu_2(Pz)]$ nodes.

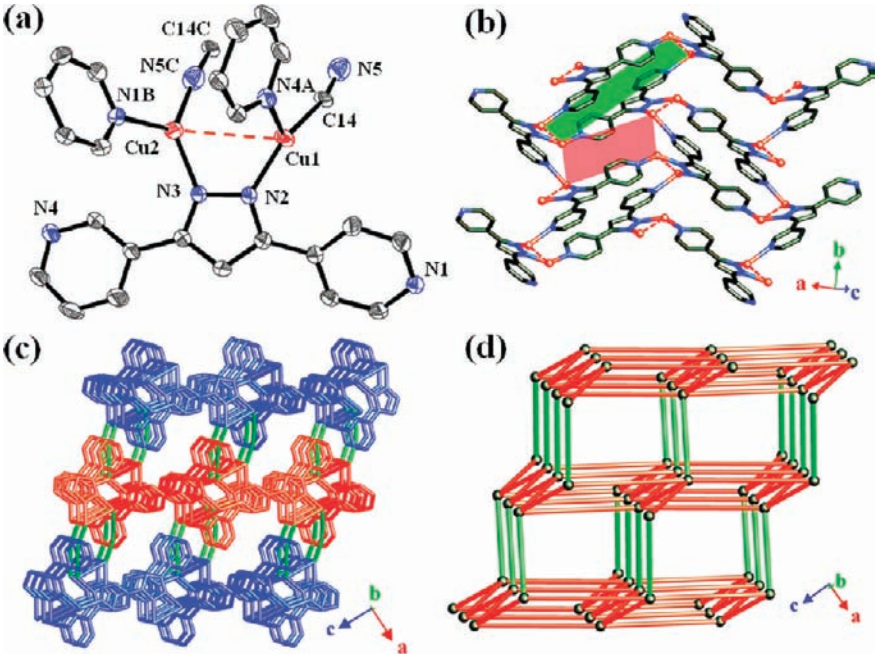

Figure 4. Structural diagrams of complex **3**: (a) ORTEP drawing of coordination environments with a 50% thermal ellipsoid; (b) layer motif of $[Cu_2(\mathbf{L3\text{-}4})]_n$ showing two kinds of four-membered rings (green and red); (c) packing diagram showing CN^- (green) connecting two 2-D layers (blue and red); (d) simplified network showing 5-connected **nov** topology; green sticks represent CN^- linkers. Symmetry codes: A, $-x + {}^1/_2, y + {}^1/_2, -z + {}^1/_2$; B, $x - {}^1/_2, -y + {}^1/_2, z + {}^1/_2$; C, $-x, -y, -z$.

*Complex **4***. The complex is a 3-D 2-fold interpenetrating polymer crystallized in the $I4_1/acd$ space group and contains one crystallographically independent Cu^I atom, half of a deprotonated **L3-3** ligand, and half of a site of one cyanide anion (Figure 5a). The Cu^I atom, adopting a distorted trigonal geometry, is coordinated by one *N*-pyrazole atom, one *N*-pyridyl atom, and one C/N atom of the cyanide anion. The deprotonated **L3-3** ligands coordinate to four symmetry-related Cu^I atoms, with the dihedral angle between the pyridyl and pyrazole rings being 32.47(1)° in the syn−syn conformation and the distance of the two Cu^I atoms bridged by the pyrazole being 3.7089(2) Å, much longer than 2.83 Å (the sum of the van der Waals radii).[31] The combination of C4 $(x + {}^1/_2, y + {}^1/_4)$ and mirror $(z + {}^1/_8)$ operations $(4/m)$ extends the asymmetry unit to a very slightly distorted tetrahedron [Figure 5b; the distances between the two Cu^I atoms connected by the cyanide anion and half of the **L3-3** ligand are 4.8983(3) and 4.8973(3) Å, respectively], in which four Cu atoms act as vertexes and two cyanide anions as well as four halves of **L3-3** ligands act as six bridges, and the C4 axis passes through the middle point of the two cyanide anions. These tetrahedral units are connected by μ_2-pyrazolate as linkers to form a 3-D framework with **dia-a** topology, in which the centers of every tetrahedron are arranged into **dia** topology or an adamantanoid cage[34] (Figure 5c,d). The large void among these tetrahedral units allows interpenetration of two equivalent frameworks. An analysis of the topology of interpenetration according to a recent classification[33b] reveals that **4** belongs to class **IIa** (Z = 2; the two interpenetrated networks are generated by center symmetry). It is noteworthy that the cyanide anions play a role of linear linkers in the *intra*framework instead of the *inter*framework of the 2-fold interpenetrated network (Figure 5e).

In order to maintain the consistency of topological simplification in this work, the $[Cu_2(Pz)]$ unit in **4** is simplified as a 6-connected node to form a new 2-fold interpenetrated 6-connected **crs** (also known as **dia-e**) network (Figure 5e; point symbol $3^6 \cdot 6^6 \cdot 7^3$; vertex symbol $3 \cdot 3 \cdot 3 \cdot 3 \cdot 3 \cdot 3 \cdot 6 \cdot 6 \cdot 6 \cdot 6 \cdot 6 \cdot 6 \cdot * \cdot * \cdot *$),[32,34,35] which is composed of tetrahedral units with a common vertex. It is the first example of an interpenetrated **crs** network (Figure 5f) according to the latest database in the *TOPOS* program.[30] As a uniform 6-connected network, the **crs** net is derived from the familiar planar 4-connected **lvt** net[34,36] (point symbol $4^2 \cdot 8^4$) through a linear linker such as the cyanide anion passing through an array of planar 4-connected nodes along the *a* and *b* axes (Figure 5e). In other words, the framework shows **lvt** topology if the cyanide anions are ignored. In fact, the **crs** net can be formed by fusing the linkers between the tetrahedra in the above **dia-a** network.

*Complex **5***. **5** is a 3-D 2-fold interpenetrated polymer constructed of the deprotonated **L4-4** ligand and CuCN. Its asymmetry unit contains one **L4-4** ligand, two cyanide anions, and three Cu^I atoms (Figure 6a). In the tetradentate deprotonated **L4-4** ligand, the two *N*-pyrazolate (N2 and N3) atoms edge-bridge Cu1 and Cu2 atoms, and the two *N*-pyridyl (N1 and N4) atoms coordinate to Cu1 and Cu3 atoms, respectively. The distance between Cu1 and Cu2 is 2.9764(5) Å, slightly longer than 2.83 Å (the sum of the van der Waals radii).[31] For the three symmetry-independent Cu^I atoms, the Cu1 atom is surrounded by one *N*-pyridyl (N1) atom, one *N*-pyrazole (N2) atom, and one cyanide anion (N6/C15) with planar trigonal geometry; the Cu3 atom is similarly surrounded by one *N*-pyridyl (N4B) atom and two cyanide anions (C15/N6 and C14C/N5C), while the Cu2 atom is linearly connected by one *N*-pyrazole (N3) atom and one cyanide anion (N5/C14). Two kinds of cyanide anions, as linear connectors, play different roles in the construction of the

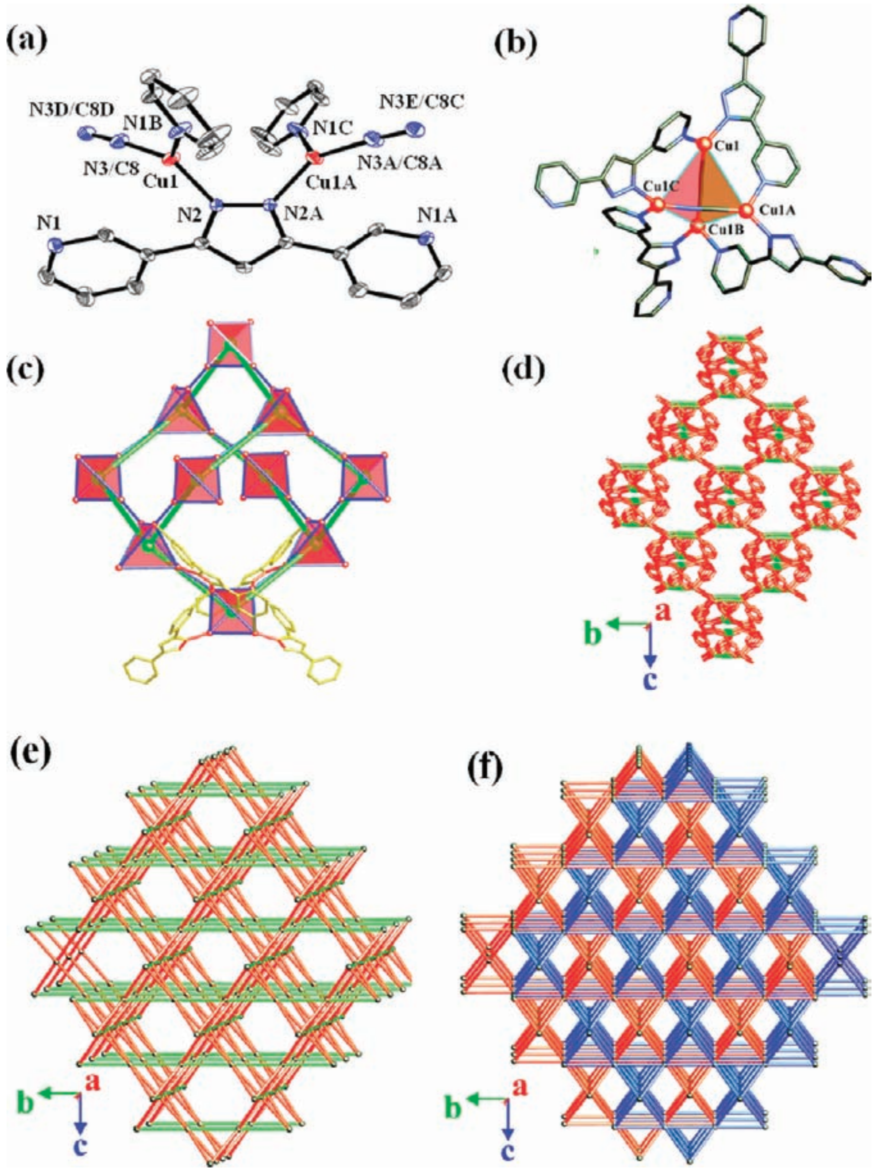

Figure 5. Structural diagrams of complex **4**: (a) ORTEP drawing of coordination environments with a 50% thermal ellipsoid; (b) tetrahedral units of four Cu atoms supported by four halves of **L3-3** ligands and two CN^- anions; (c) an adamantanoid cage (blue) constructed by tetrahedral units showing **dia-a** topology (green denoted as the **dia** network); (d) perspective of a single framework (CN^- anions represented by green bonds); (e) single framework showing **dia-e** topology; green sticks represent CN^- linkers. (f) 3-D interpenetrated topology network. Symmetry codes: (a) A, $-x + {}^{1}/_{2}$, y, $-z$; B, $-y + {}^{3}/_{4}$, $x - {}^{1}/_{4}$, $-z + {}^{1}/_{4}$; C, $y - {}^{1}/_{4}$, $x - {}^{1}/_{4}$, $z - {}^{1}/_{4}$; D, $-x + 1$, $-y + {}^{1}/_{2}$, z; E, $x - {}^{1}/_{2}$, $-y + {}^{1}/_{2}$, $-z$; (b) A, $y + {}^{1}/_{4}$, $-x + {}^{3}/_{4}$, $-z + {}^{1}/_{4}$; B, $-x + 1$, $-y + {}^{1}/_{2}$, z; C, $-y + {}^{3}/_{4}$, $x - {}^{1}/_{4}$, $-z + {}^{1}/_{4}$.

3-D structures (Figure 6b,c). The first kind, N5C14, connects two **L4-4** ligands through four Cu2 and Cu3 atoms, resulting in a tetragonal unit (green shadow in Figure 6b) of $[Cu_4(\mathbf{L4\text{-}4})_2(CN)_2]$ with four Cu atoms (two Cu2 and two Cu3 atoms) as vertexes and the cyanide anions as well as two half-parts of **L4-4** as edges. These tetragonal units are united by the third kind of Cu atoms (Cu1) to form a 2-D layer cationic subnet of $[Cu_3(\mathbf{L4\text{-}4})(CN)]_n$, in which the third coordination bonds of Cu1 and Cu3 atoms stay vacant (Figure 6b). The second kind of cyanide anions, N6C15, connects such adjacent layer subnets from two sides via the third vacant coordination site of the Cu1 and Cu3 atoms to form a 3-D framework (Figure 6c). The large void supported by the long linear **L4-4** ligands allows two identical networks to interpenetrate with each other, and the resulting 2-fold interpenetrating network belongs to class **Ia**[33b] (all of the interpenetrated nets are generated only by translationm and the translation vector is [100] 5.69 Å). By assigning the $[Cu_2(Pz)]$ units as 5-connected nodes, the 2-fold interpenetrating framework shows a 3,5-connected binodal topology (Figure 6d) with point symbol $(4\cdot6^2)(4\cdot6^7\cdot8^2)$ and vertex symbol $(4\cdot6_2\cdot6_2)(4\cdot6\cdot6\cdot6\cdot6\cdot6\cdot6\cdot6_2\cdot8_2\cdot8_3)$,[33,34,36] known to *TOPOS*[30] and called **seh-3,5-P21/c** arising from two works on the generation of uninodal and binodal nets.[37]

*Complexes **6-Br** and **6-Cl**.* Isostructural complexes **6-Br** and **6-Cl** were obtained by reacting H**L4-4** and corresponding bivalent copper salts ($CuBr_2$/$CuCl_2$), which were reduced to monovalent Cu^I in solvothermal conditions.[24,38] The asymmetric unit contains one deprotonated **L4-4** ligand, one halide anion Br1/Cl1, two Cu^I atoms (Cu1 and Cu2) doubly bridged by

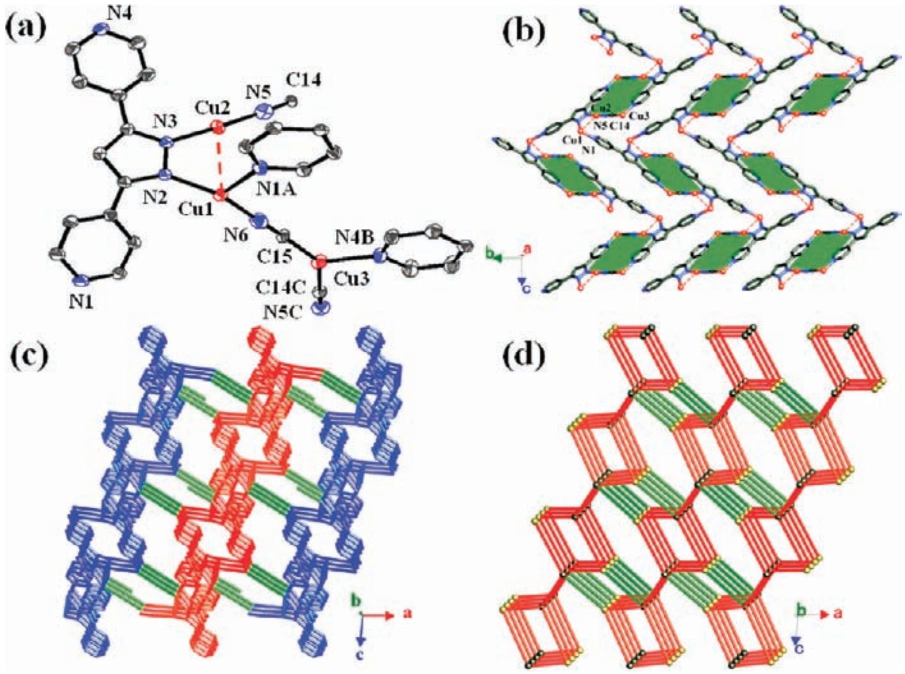

Figure 6. Structural diagrams of complex **5**: (a) ORTEP drawing of coordination environments with a 50% thermal ellipsoid; (b) 2-D layer cationic subnet; (c) 3-D single framework constructed of CN^- (N6C15, green) linking a 2-D layer cationic subnet; (d) topology network of a single framework. Symmetry codes: A, $-x + {}^3/_2, y + {}^1/_2, -z + {}^1/_2$; B, $x + {}^3/_2, -y + {}^3/_2, z + {}^1/_2$; C, $-x + {}^7/_2, y - {}^1/_2, -z + {}^1/_2$.

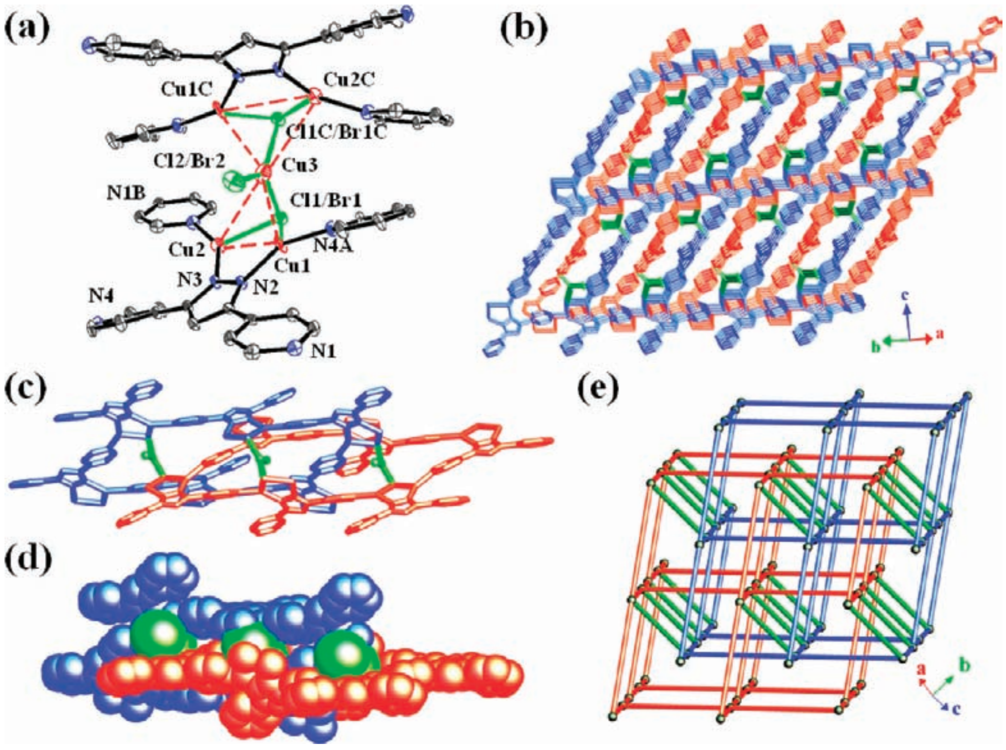

Figure 7. Structural diagrams of complexes **6-Br** and **6-Cl**: (a) ORTEP drawing of coordination environments with a 50% thermal ellipsoid; (b) perspective of self-catenated frameworks constructed by $[CuX_3]$ units (green) cross-linking two interpenetrated frameworks (red and blue); (c) stick and (d) filling diagrams of self-catenated fragments; (e) schematic view of a $4^2 \cdot 6^7 \cdot 8$ self-catenated topological network constructed by linkers (green) cross-linking interpenetrated **cds** networks (red and blue). Symmetry codes: A, $x + {}^1/_2, -y + {}^1/_2, z + {}^1/_2$; B, $x - {}^1/_2, y + {}^1/_2, z$; C, $-x, y, -z + {}^3/_2$.

pyrazolate and a Br1/Cl1 anion, as well as a neutral CuX (Cu3Br2/Cu3Cl2) fragment with ${}^1/_2$ site occupancy (Figure 7a).

The neutral CuX fragment is located at the 2-fold symmetry axis paralleling the *b* axis, playing the role of linker connecting two

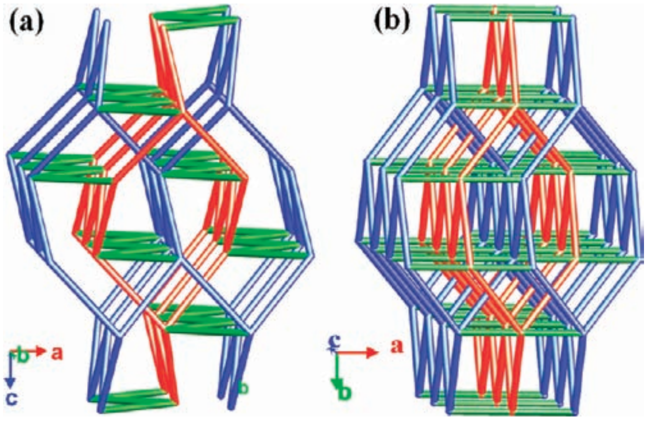

Figure 8. Schematic views of polyknotted topology networks constructed by linkers (green) cross-linking interpenetrated **dia** networks (red and blue) with different linkage modes for **7α-SCN**: **7α-N$_3$** (a) and **7*β*-SCN** (b).

symmetry-related [Cu$_2$(μ_2-X)(**L4-4**)] units through the coordination bond of Cu3−Br1/Cu3−Cl1 with a distance of 2.3931(5)/2.2831(8) Å (Figure 7a). In the two complexes, all Cu atoms adopt distorted triangular geometry. Cu1 and Cu2 are coordinated by one *N*-pyrazolate atom, one *N*-pyridyl atom, and the same Br/Cl atom, while Cu3 is coordinated by three Br/Cl atoms, one of which acts as a terminal ligand (Br2/Cl2), and the other two are symmetry-related Br1/Cl1 and Br1C/Cl1C. Additionally, the distances between these Cu atoms range from 2.8319(5) to 3.5531(1) Å, indicating different Cu···Cu weak interactions. Compared to complex **6-Br**, the distances of Cu−Cu, Cu−X, and Cu−N in complex **6-Cl** are slightly shorter (Table S1 in the Supporting Information), perhaps because of the smaller radius of the Cl$^-$ anion.

Through the symmetry operations, the two fragments, [Cu$_2$(μ_2-Br)(**L4-4**)]/[Cu$_2$(μ_2-Cl)(**L4-4**)], in **6-Br** and **6-Cl** connected by Cu3Br2/Cu3Cl2 are extended to two identical 3-D 2-fold interpenetrated infinite frameworks, which are, in fact, symmetrical about the only C2 axis (parallel to the *b* axis) in a monoclinic crystal system (Figure 7b). The generation of interpenetration can obviously be ascribed to the long linear ligands supporting large voids. Topological analysis of the interpenetration reveals that they belong to class **IIa**[33b] ($Z = 2$; the two interpenetrated networks are generated by center symmetry), similar to that of complex **4**. Each 3-D infinite framework can be rationally collapsed to a familiar **cds** (CdSO$_4$) topological network (point symbol $6^5 \cdot 8$)[34,39] by viewing the center of every [Cu$_2$(μ_2-Br)(μ_2-Pz)]/[Cu$_2$(μ_2-Cl)(μ_2-Pz)] unit as a planar 4-connected node. The Cu3Br2/Cu3Cl2 fragments, acting as bridges, connect two interpenetrated 3-D networks to form an inseparable whole. The whole network is a uniform 5-connected self-catenated network with point symbol $4^2 \cdot 6^7 \cdot 8$ (vertex symbol $4 \cdot 4 \cdot 6_2 \cdot 6_3 \cdot 6_3 \cdot 6_3 \cdot 6_3 \cdot 6_4 \cdot 6_4 \cdot *$)[34,35] (Figure 7e), which is a known uninodal 5-connected net called "**hxg-d-5-C2/c**" by *TOPOS*,[30] meaning that it is derived from the 10-coordinated **hxg-d** net.[37]

We can clearly see that two interpenetrated six-membered rings are connected by three Cu3Br2/Cu3Cl2 fragments as linkers (Figure 7c,d), and one of the shortest circuits (six-membered, red or blue) is threaded by a connection (blue or red), which is from the same network containing the shortest circuits. Therefore, **6-Br** and **6-Cl** represent classical 3-D self-catenated nets constructed by coordination bonds.[9,34,35]

Complexes ***7α-SCN*** *and* ***7β-SCN***. As previously communicated,[11a] **7α-SCN** and **7*β*-SCN** are rarely observed topological self-catenated isomers constructed by deprotonated **L4-4** and CuSCN, wherein the **L4-4** ligands and Cu atoms construct the two interpenetrated frameworks and the thiocyanate anions act as connectors in the cross-linking of these two interpenetrated frameworks to form an inseparable whole, therefore generating self-catenated complexes (Figure 8). The main difference between them is the linkage modes of the thiocyanate anions: ziazag mode for **7α-SCN** and linear mode for **7*β*-SCN**. It is such different linkage modes that lead to generation of the novel self-catenated isomers of **7α-SCN** and **7*β*-SCN**.

In our previous communication,[11a] we described the two complexes as 3,5-binodal polyknotted isomers based on 2-fold interpenetrated **srs**-(**10^3-a**) and **ths**-(**10^3-b**) nets by assigning the pyrazolate ring and two doubly bridged Cu centers as 3- and 5-connected nodes, respectively. In order to keep consistency with the above topological assignments, herein we assign the center of [Cu$_2$(μ_2-S)(μ_2-Pz)] to a node, and hence the two isomers are simplified to different uniform 6-connected self-catenated networks with the same point symbol $4^8 \cdot 6^7$ but with different vertex symbols.[34,35] The vertex symbol of **7α-SCN** is $4 \cdot 4 \cdot 4 \cdot 4 \cdot 4 \cdot 4 \cdot 4 \cdot 4 \cdot 6_3 \cdot 6_3 \cdot 6_4 \cdot 6_4 \cdot 6_8 \cdot 6_9 \cdot 6_9$, which is a known uninodal 6-connected net called "**cco-6-Pbcm**" by *TOPOS*,[30] meaning that it is derived from the familiar 10-coordinated **cco** net,[37] while the vertex symbol of **7*β*-SCN** is $4 \cdot 4 \cdot 4 \cdot 4 \cdot 4 \cdot 4 \cdot 4 \cdot 4 \cdot 6_2 \cdot 6_2 \cdot 6_4 \cdot 6_8 \cdot 6_8 \cdot 6_8 \cdot 6_8$, a known net called **msw**.[36c] The two nets are based on two interpenetrated **dia** (diamond) frameworks cross-linked by thiocyanate anions in different modes. Topological analysis[33b] of the interpenetration reveals that they belong to class **IIa** ($Z = 2$; the two interpenetrated networks are generated by center symmetry), similar to complexes **4** and **6**. This assignment is rational because 3-connected **srs**-(**10^3-a**) and **ths**-(**10^3-b**) networks can be converted to a 4-connected **dia** network by fusing two 3-connected nodes to a single 4-connected node,[9a] and therefore the two 3,5-binodal self-catenated networks can also be converted to 6-connected polyknotted networks by fusing the 3- and 5-connected nodes together to a single 6-connected node. To the best of our knowledge, complexes **7α-SCN** and **7*β*-SCN** represent a new polyknotted isomerism. The analogues of a 6-connected $4^8 \cdot 6^7$ topological self-catenated network based on multifold interpenetrated **dia** networks were reported earlier,[10c] but **7α-SCN** and **7*β*-SCN** exhibit two new 6-connected uniform polyknotted topology networks when the vertex symbol is taken for consideration.

Complex ***7α-N$_3$***. The complex is an isostructure of complex **7α-SCN**. In complex **7α-N$_3$**, N$_3^-$ adopts the frequently observed (μ-1,1,3) modes connecting three Cu$^{\mathrm{I}}$ atoms, replacing the position of SCN$^-$ in **7α-SCN**, and acting as linkers to cross-link two interpenetrated networks to form a self-catenated network. In the complex, the N$_3^-$ anion retains its delocalized electronic configuration and the triple bonds among the three N atoms because the distances of N5−N6 and N6−N7 are about 1.15 Å, very similar to that in solid inorganic salt NaN$_3$.[40] Perhaps there are only subtle differences between the two N−N bonds caused by the perturbation of the chemical environments of the two terminal N atoms (N5 and N7), which is further supported by IR spectra splitting into two parts (2055 and 2038 cm^{-1}) in the N$_3^-$ anion characteristic absorption region. Additionally,

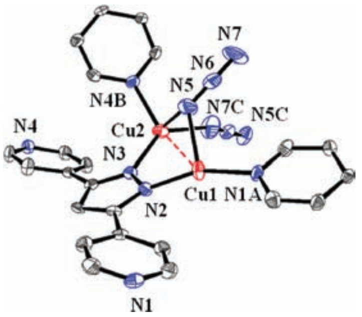

Figure 9. ORTEP drawing of coordination environments with a 50% thermal ellipsoid for **7α-N$_3$**. Symmetry codes: A, $x + {}^1/_2$, $-y + {}^5/_2$, $-z + 1$; B, $-x + 2$, $y + {}^1/_2$, $-z + {}^1/_2$; C, $-x + {}^5/_2$, $y - {}^1/_2$, z.

such an electronic configuration makes the length of the N_3^- anion (about 2.34 Å) a little shorter than that of SCN^- (2.78 Å), which reduces the *a* axis lengths and the cell volumes (from 12.365 Å and 2802 Å^3 in **7α-SCN** to 11.398 Å and 2609 Å^3 in **7α-N$_3$**; see Figure 9) and increases the packing density.

Second Ligating Spacers. Complexes **1**−**7** show structural evolution from 1-D to 3-D self-catenated isostructural/isomeric systems. Except for **5**, these complexes exhibit very similar coordination environments of Cu^I atoms and pyridylpyrazolate ligands: two Cu^I atoms edge-bridged by the deprotonated pyrazolate ring are further coordinated by the side-armed pyridyl ring to construct 1-D, 2-D, and 3-D interpenetrated (but not self-catenated) frameworks based on the $[Cu_2(\mu_2\text{-Pz})]$ units as 4-connected nodes (Figure 10 and Table 2). The 4-connected networks vary from 2-D regular and irregular $4^4 \cdot 6^2$ layers to 3-D noninterpenetrated and interpenetrated **lvt**, **cds**, and **dia** topology because of various auxiliary anionic ligands and variation of the pyridylpyrazolate ligands. The generation of interpenetration is related closely to the length of these ligands, which is consistent not only with our anticipation but also with previous conclusions.[9a−c] Ligated by halide and pseudohalide anion spacers, these compounds show a transition from 1-D to 3-D and from nonentanglements to self-catenated isostructures/isomers. Their chemical composition, catenations, point symbol, and other information are summarized in Table 2. Besides variation of the **L3-3**, **L3-4**, and **L4-4** ligands, the auxiliary anionic ligands play key roles for construction of these catenated systems. They act not only as charge balances but also as ligating spacer *inter-* or *intra*linking $[Cu_2(\mu_2\text{-Pz})]$ units. The various coordination modes (electronic conformation) and ionic shape of these auxiliary anionic ligands lead to their various functions. Importantly, the distinct characteristics of these analogous self-catenated complexes compared with those reported are that they are based on interpenetration networks; in other words, they are generated through the cross-linking of two interpenetrated frameworks via bridging connector fragments to form inseparable wholes, the so-called self-catenation.

Halide, SCN^-, and N_3^- anions can further bridge the two Cu^I atoms in the Cu_2-pyrazolated units (observed in **1**, **2-Br**, **2-Cl**, **6-Br**, **6-Cl**, **7α-SCN**, ***7β*-SCN**, and **7α-N$_3$**) because the coordinating atoms in these anions contain at least two pairs of σ electrons, which results in the distance between the two atoms bridged by them coinciding with that by pyrazolate. However, this is not the case for the CN^- anion. Though the μ_2-N or μ_2-C bridging mode for CN^- is very common, the distance between the two Cu atoms (usually less than 2.6 Å) bridged by CN^- is much shorter than that in $[Cu_2(\mu_2\text{-Pz})]$ unit (usually more than 2.8 Å). This may be due to there being only one pair of σ electrons in the C/N atom of CN^-, which leads to the inconsistency for the formation of the doubly bridging modes by pyrazolate and μ_2-N/C from the CN^- anion. In fact, in complexes **3**−**5**, the CN^- anion connects two distinct Cu^I atoms via the μ_2-(C,N) linear mode.

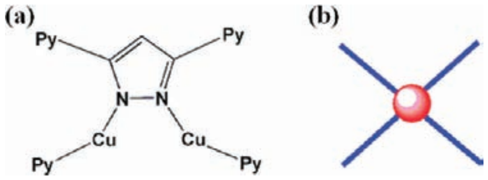

Figure 10. Coordination environments of the pyridylpyrazolate ligands (a) and a related simplified 4-connected node (b).

Halide anions are a kind of monatomic auxiliary anionic ligand with small size (or small steric crowd) and more donor electrons for coordination.[25] In **1**, **2-Br**, and **3-Cl**, I^-, Br^-, and Cl^- anions act only as μ_2 bridges to construct the doubly bridged binuclear units $[Cu_2(Pz)X]$. The excess lone-pair electrons provide the possibility of coordinating to more Cu atoms via μ_3 and μ_4 modes. Therefore, it is reasonable that the Br1 and Cl1 atoms coordinate to the third Cu atoms of the CuBr and CuCl fragments in complexes **6-Br** and **6-Cl**. It is the third coordination bonds of the halides cross-linking two interpenetrating **cds** networks that result in the unusual self-catenated structures of **6-Br** and **6-Cl**.

The analogous self-catenated structures are well represented by **7α-SCN**, ***7β*-SCN**, and **7α-N$_3$**. Compared with halide anions and CN^-, SCN^- and N_3^- anions exhibit longer shape and various coordination modes. Their shape and electronic configuration are suitable for bridging two Cu^I atoms in the $[Cu_2(\mu_2\text{-Pz})]$ unit via the μ_2-S atom and further bridging two $[Cu_2(\mu_2\text{-Pz})]$ units by a linear bidentate μ_2-(S,N) mode. In **7α-SCN** and ***7β*-SCN**, SCN^- anions act as bridges cross-linking two interpenetrated structures, giving rise to self-catenated structures based on 2-fold interpenetrated **dia** networks. Interestingly, two different linkage modes result in two unprecedented self-catenated topological isomers, **7α-SCN** and ***7β*-SCN**. The N_3^- anion is introduced because of its analogous space and electronic configuration compared with those of SCN^-. In **7α-N$_3$**, an isostructure of **7α-SCN**, the N_3^- anions show the same coordination mode and play the same role as SCN^- in **7α-SCN**. Unfortunately, attempts to obtain ***7β*-N$_3$**, the isostructure of ***7β*-SCN**, have not been successful so far.

CN^- is a good linear ligating spacer. In complexes **3**−**5**, all of the CN^- anions show the μ_2-(C,N) bridging modes, but their roles are diverse in the construction of these 3-D structures. In complex **3**, a pair of CN^- anions act as linkers connecting two $[Cu_2(\mu_2\text{-Pz})]$ units in the 2-D sheets, extending to a 3-D structure. In complex **4**, each CN^- anion acts as a linker connecting two $[Cu_2(\mu_2\text{-Pz})]$ units within one single net, instead of *inter*linking the two interpenetrated frameworks, resulting in 2-fold interpenetration instead of self-catenation. In complex **5**, two kinds of CN^- anions play two roles, namely, *intra-* and *inter*linking modes, resulting in two 3-D interpenetrated frameworks but not a self-catenated net. Great efforts were paid to pursue self-catenated structures based on interpenetrated networks cross-linked by CN^- anions, without success so far. Perhaps the length and electronic configuration of CN^- are not suitable for the cross-linking of two interpenetrating networks into one whole.

Table 2. Brief Summary of the Structural Features of Complexes **1**−**7**

complex	composition	ligand	anion	dimension	catenation	point symbol[a] a	point symbol[a] b
1	Cu_2(**L3-3**)I	**L3-3**	I^-	1-D	no		
2-Br	Cu_2(**L4-4**)Br	**L4-4**	Br^-	2-D	no	4^4-**sql**	4^4-**sql**
2-Cl	Cu_2(**L4-4**)Cl	**L4-4**	Cl^-	2-D	no	4^4-**sql**	4^4-**sql**
3	Cu_2(**L3-4**)(CN)	**L3-4**	CN^-	3-D	no	4^4-**sql**	$4^4 \cdot 6^6$-**nov**
4	Cu_2(**L3-3**)(CN)	**L3-3**	CN^-	3-D	2-fold	$4^2 \cdot 8^4$-**lvt**	$3^6 \cdot 6^6 \cdot 7^3$-**crs**
5	Cu_3(**L4-4**)$(CN)_2$	**L4-4**	CN^-	3-D	2-fold		$(4 \cdot 6^2)(4 \cdot 6^7 \cdot 8^2)$
6-Br	$[Cu_2$(**L4-4**)$]_2(CuBr_3)$	**L4-4**	Br^-	3-D	self-catenated	$6^5 \cdot 8$-**cds**	$4^2 \cdot 6^7 \cdot 8$
6-Cl	$[Cu_2$(**L4-4**)$]_2(CuCl_3)$	**L4-4**	Cl^-	3-D	self-catenated	$6^5 \cdot 8$-**cds**	$4^2 \cdot 6^7 \cdot 8$
7α-SCN	Cu_2(**L4-4**)(SCN)	**L4-4**	SCN^-	3-D	self-catenated	6^6-**dia**	$4^8 \cdot 6^7$ [b]
7*β*-SCN	Cu_2(**L4-4**)(SCN)	**L4-4**	SCN^-	3-D	self-catenated	6^6-**dia**	$4^8 \cdot 6^7$ [c]
7α-N₃	Cu_2(**L4-4**)(N_3)	**L4-4**	N_3^-	3-D	self-catenated	6^6-**dia**	$4^8 \cdot 6^7$ [c]

[a] (a) Simplified networks of the $[Cu_2L]_n$ frameworks (not including second ligating spacers); (b) simplified networks of the overall complexes. [b] Vertex symbol $4 \cdot 4 \cdot 4 \cdot 4 \cdot 4 \cdot 4 \cdot 4 \cdot 4 \cdot 6_3 \cdot 6_3 \cdot 6_4 \cdot 6_4 \cdot 6_8 \cdot 6_9 \cdot 6_9$. [c] Vertex symbol $4 \cdot 4 \cdot 4 \cdot 4 \cdot 4 \cdot 4 \cdot 4 \cdot 4 \cdot 6_2 \cdot 6_2 \cdot 6_4 \cdot 6_8 \cdot 6_8 \cdot 6_8 \cdot 6_8$.

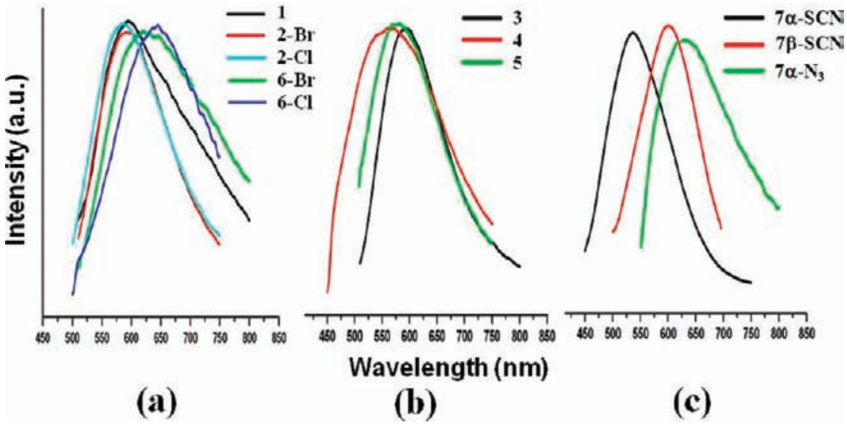

Figure 11. Solid-state luminescence spectra of complexes **1**−**7** at room temperature.

Luminescence Properties. Complexes **1**−**7** show strong photoluminescence properties from yellow to red upon excitation by UV light in the solid state at room temperature (Figure 11). The emission maxima (λ_{em}^{max}) and corresponding excitation maxima (λ_{ex}^{max}) are listed in Table 3. Figure 11 shows their emission spectra categorized according to the second ligating spacers. The coordination environments of Cu^I centers in these complexes are similar, which warrants the similar luminescence origins of charge transfers between metals and ligands. The variations of their luminescence properties are mainly caused by the second ligating ligands, which is important for the structure luminescence investigation and comparison of coordination polymer systems.

According to previous literature,[19,26,41] we tentatively assigned all of the emissions to mainly originate from ^{3}[MLCT] excited states because of their broad and structureless emission spectra. This attribution is also supported by a luminescence investigation on nonaromatic-group-substituted pyrazolate-based copper(I) complexes.[22] In comparison, the pyridyl-substituted pyrazolate ligands in this work are a series of large π systems with lower energy of the π^* orbital, which are more favorable for MLCT. Although all Cu···Cu distances bridged by pyrazolate are longer than the sum of the van der Waals radii,[31] they all fall within the possible range of cuprophilic interaction.[5d,41] Therefore, the Cu···Cu weak interactions may more or less contribute to the emissions.

Table 3. Luminescence Data of Complexes **1**−**7**

complex	λ_{ex}^{max} (nm)	λ_{em}^{max} (nm)	possible origins
1	370	593	MLCT, XMCT
2-Br	427	591	MLCT, XMCT
2-Cl	368	580	MLCT, XMCT
3	422	592	MLCT, MMLCT
4	372	562	MLCT
5	367	580	MLCT, MMLCT
6-Br	375	620	MLCT, MC, XMCT
6-Cl	372	640	MLCT, MC, XMCT
7α-SCN	440	598	MLCT, XMCT
7*β*-SCN	398	537	MLCT, XMCT
7α-N₃	480	627	MLCT

Complexes **1**, **2-Br**, **2-Cl**, **6-Br**, and **6-Cl**, all containing halide anions as second ligating spacers, exhibit orange to red emission bands with maxima larger than 580 nm. Such low-energy emission may be assigned to MLCT mixed with XMCT but without XLCT.[19c,26a] The coordination environments of **1**, **2-Br**, and **2-Cl** are similar, but their emission maxima are 593, 591, and 580 nm, respectively, following the electronegativity order of I < Br < Cl. The slight blue shift may be caused by the electron-withdrawing effects of the halide atoms: the stronger the electronegativites, the more disfavorable the $Cu^I \rightarrow L$ electron donation. Compared to **1**, **2-Br**, and **2-Cl**, the red shifts (larger than 30 nm) of **6-Br** and **6-Cl** are perhaps related closely to the shorter Cu···Cu distance (about 2.83 Å, comparable to the sum of the van der Waals radii[31]). Also, the lower emission of **6-Cl** (λ_{ex}^{max} = 640 nm) may be related to its much shorter Cu···Cu distance in **6-Cl** compared to **6-Br**. Therefore, the excited states of MC or metal–metal-to-ligand charge transfer (MMLCT) should be taken into consideration for the luminescence origins of **6-Br** and **6-Cl**.[19c,26a] Also, the possibility of XMCT cannot be excluded.

The emission peaks of complexes **3**–**5** with cyanide anions are more or less higher energy than others. Such a tendency is reasonable because the CN^- anion is an electron acceptor instead of a donor, compared with halide and SCN^-. The lower emission energy of **3** and **5** than that of **4** may originate from the shorter Cu···Cu distances. So, MMLCT should not be excluded. The much weaker emission intensity and higher emission energy of **4** compared to those of **3** and **5** (the intensity is normalized in Figure 11) may be ascribed to the largest dihedral angles between the pyridyl and pyrazolate planes in **4** (Table S1 in the Supporting Information and Figure 5), which makes conjugation of the ligand severely disrupted.

In our previous communication,[11a] the emissions of **7α-SCN** and **7*β*-SCN** were assigned to a mixture of XMCT (S → Cu) and MC modified by Cu···Cu weak interactions. Herein, by comparing with the emission spectra of other complexes, MLCT may also be involved. However, **7α-N$_3$** exhibits much lower energy excitation and emission bands (λ_{ex}^{max} = 480 nm, λ_{em}^{max} = 627 nm, red emission) than its isostructure **7α-SCN** (λ_{ex}^{max} = 440 nm, λ_{em}^{max} = 598 nm, yellow emission). Taking into consideration the π conjugation of the N_3^- anion, another MLCT from the d electron of the Cu^I centers to the π^* orbitals of the N_3^- anion may be responsible for such a red shift. Further investigation is needed to clarify the luminescence origins in this system.

CONCLUSION

In summary, these complexes show a topological evolution from a 1-D to 3-D increase, especially from interpenetration to self-catenation for the 3-D isomers/isostructures. Most of these complexes are based on 4-connected networks constructed by the $[Cu_2(Pz)]$ units. The introduction of appropriate linear second ligating spacers, halides, and pseudohalides, acting as bridges to the *inter-* or *intra*linking interpenetrating framework, generates highly sophisticated structures such as self-catenated nets and even self-catenated isomers. Though generation of these self-catenated structures, especially for the self-catenated isomers, is unpredictable, the results provide some clues to rationally design and synthesize novel self-catenated architectures including self-catenated isomers.

Moreover, photoluminescence studies indicate that the emissions of these complexes mainly originate from ^{3}[MLCT] excited states modified by weak cuprophilic interactions and also are affected by the electron effects of the second ligating ligands of halides and pseudohalides. These results establish a strategy for understanding the structure–property relationship, especially for the luminescence variation and origin, by systematically investigating the subtle structural differences in isomeric and isostructural luminescent coordination polymers.

ASSOCIATED CONTENT

Supporting Information. Crystallographic data in CIF format for these structures, selected bond lengths and bond angles, PXRD patterns, and TGA curves. This material is available free of charge via the Internet at http://pubs.acs.org.

AUTHOR INFORMATION

Corresponding Author

*E-mail: dli@stu.edu.cn.

ACKNOWLEDGMENT

This work was financially supported by the National Science Foundation for Distinguished Young Scholars of China (Grant 20825102) and the National Natural Science Foundation of China (Grant 20771072).

REFERENCES

(1) (a) Robson, R.; Abrahams, B. F.; Batten, S. R.; Gable, R. W.; Hoskins, B. F.; Liu, J. *Supramolecular Architecture*; American Chemical Society: Washington, DC, 1992; p 256. (b) Lehn, J. M. *Supramolecular Chemstry: Concepts and Perspectives*; VCH: Weinheim, Germany, 1995; Chapter 9. (c) Steed, J. W.; Atwood, J. L. *Supramolecular Chemistry*; Wiley: Chichester, U.K., 2000. (d) Subramanian, S.; Zaworotko, M. *Coord. Chem. Rev.* **1994**, *127*, 357. (e) Fredericks; J. R.; Hamilton, A. D. In *Comprehensive Supramolecular Chemistry*; Stang, J. P., Hosseini, M. W., Eds.; Pergamon: Oxford, U.K., 1996; Vol. 9, Chapter 16.

(2) (a) Leininger, S.; Olenyuk, B.; Stang, P. J. *Chem. Rev.* **2000**, *100*, 853. (b) Seidel, S. R.; Stang, P. J. *Acc. Chem. Res.* **2002**, *35*, 972. (c) Fujita, M.; Tominaga, M.; Hori, A.; Therrien, B. *Acc. Chem. Res.* **2005**, *38*, 371. (d) Fiedler, D.; Leung, D. H.; Bergman, R. G.; Raymond, K. N. *Acc. Chem. Res.* **2005**, *38*, 351. (e) Lee, S. J.; Lin, W. *Acc. Chem. Res.* **2008**, *41*, 521.

(3) For example: (a) Eddaoudi, M.; Kim, J.; Rosi, N. L.; Vodak, D. T.; Wachter, J.; O'Keeffe, M.; Yaghi, O. M. *Science* **2002**, *295*, 469. (b) Yaghi, O. M.; O'Keeffe, M.; Ockwig, N. W.; Chae, H. K.; Eddaoudi, M.; Kim, J. *Nature* **2003**, *423*, 705. (c) Rosi, N. L.; Eddaoudi, M.; Vodak, D. T.; Eckert, J.; O'Keeffe, M.; Yaghi, O. M. *Science* **2003**, *300*, 1127. (d) Chae, H. K.; Siberio-Pérez, D. Y.; Kim, J.; Go, Y.; Eddaoudi, M.; Matzger, A. J.; O'Keeffe, M.; Yaghi, O. M. *Nature* **2004**, *427*, 523. (e) Rowsell, J. L. C.; Spencer, E. C.; Eckert, J.; Howard, J. A. K.; Yaghi, O. M. *Science* **2005**, *309*, 1350. (f) Deng, H.; Doonan, C. J.; Furukawa, H.; Ferreira, R. B.; Towne, J.; Knobler, C. B.; Wang, B.; Yaghi, O. M. *Science* **2010**, *327*, 846. (g) Tranchemontagne, D. J.; Mendoza-Cortés, J. L.; O'Keeffe, M.; Yaghi, O. M. *Chem. Soc. Rev.* **2009**, *38*, 1257.

(4) (a) Zhang, J.-P.; Chen, X. M. *J. Am. Chem. Soc.* **2008**, *130*, 6010. (b) Zhang, J.-P.; Chen, X.-M. *J. Am. Chem. Soc.* **2009**, *131*, 5516. (c) Wang, X.-L.; Qin, C.; Wu, S.-X.; Shao, K. Z.; Lan, Y. Q.; Wang, S.; Zhu, D. X.; Su, Z. M.; Wang, E. B. *Angew. Chem., Int. Ed.* **2009**, *48*, 5291. (d) Neville, S. M.; Halder, G. J.; Chapman, K. W.; Duriska, M. B.; Moubaraki, B.; Murray, K. S.; Kepert, C. J. *J. Am. Chem. Soc.* **2009**, *131*, 12106. (e) Wang, X. S.; Ma, S.; Rauch, K.; Simmons, J. M.; Yuan, D.; Wang, X.; Yildirim, T.; Cole, W. C.; López, J. J.; Meijere, A. D.; Zhou, H. C. *Chem. Mater.* **2008**, *20*, 3145. (f) Bae, Y. S.; Dubbeldam, D.; Nelson, A.; Walton, K. S.; Hupp, J. T.; Snurr, R. Q. *Chem. Mater.* **2009**, *21*, 4768. (g) Kanoo, P.; Matsuda, R.; Higuchi, M.; Kitagawa, S.; Maji, T. K. *Chem. Mater.* **2009**, *21*, 5860.

(5) (a) Moulton, B.; Zaworotko, M. J. *Chem. Rev.* **2001**, *101*, 1629. (b) Abourahma, H.; Moulton, B.; Kravtsov, V.; Zaworotko, M. J. *J. Am. Chem. Soc.* **2002**, *124*, 9990. (c) Huang, X.-C.; Zhang, J.-P.; Chen, X.-M. *J. Am. Chem. Soc.* **2004**, *126*, 13218. (d) Zhang, J.-P.; Lin, Y.-Y.; Huang, X.-C.; Chen, X.-M. *Dalton Trans.* **2005**, 3681. (e) Zhang, J.-P.; Huang, X.-C.; Chen, X.-M. *Chem. Soc. Rev.* **2009**, *38*, 2385.

(6) (a) Ma, S.; Sun, D.; Ambrogio, M. W.; Fillinger, J. A.; Parkin, S.; Zhou, H. C. *J. Am. Chem. Soc.* **2007**, *129*, 1858. (b) Shekhah, O.; Wang, H.; Kowarik, S.; Schreiber, F.; Paulus, M.; Tolan, M.; Sternemann, C.; Evers, F.; Zacher, D.; Fischer, R. A.; Woll, C. *J. Am. Chem. Soc.* **2007**, *129*, 15118. (c) Zhang, J. J.; Wojtas, L.; Larsen, R. W.; Eddaoudi, M.; Zaworotko, M. J. *J. Am. Chem. Soc.* **2009**, *131*, 17040. (d) Farha, O. K.; Malliakas, C. D.; Kanatzidis, M. G.; Hupp, J. T. *J. Am. Chem. Soc.* **2010**, *132*, 950. (e) Bureekaew, S.; Sato, H.; Matsuda, R.; Kubota, Y.; Hirose, R.; Kim, J.; Kato, K.; Takata, M.; Kitagawa, S. *Angew. Chem., Int. Ed.* **2010**, *49*, 7660. (f) Deshpande, R. K.; Minnaar, J. L.; Telfer, S. G. *Angew. Chem., Int. Ed.* **2010**, *49*, 4598.

(7) (a) Pease, A. R.; Jeppesen, J. O.; Stoddart, J. F.; Luo, Y.; Collier, C. P.; Heath, J. R. *Acc. Chem. Res.* **2001**, *34*, 433. (b) Collin, J. P.; Diertrich-Buchecker, C.; Gaviña, P.; Jimenez-Molero, M. C.; Sauvage, J. P. *Acc. Chem. Res.* **2001**, *34*, 477. (c) Schalley, C. A.; Beizai, K.; Vögtle, F. *Acc. Chem. Res.* **2001**, *34*, 465. (d) Ballardini, R.; Balzani, V.; Credi, A.; Gandolfi, M. T.; Venture, M. *Acc. Chem. Res.* **2001**, *34*, 445. (e) Cantrill, S. J.; Chichak, K. S.; Peters, A. J.; Stoddart, J. F. *Acc. Chem. Res.* **2005**, *38*, 1. (f) Harada, A.; Hashidzume, A.; Yamaguchi, H.; Takashima, Y. *Chem. Rev.* **2009**, *109*, 5974. (g) Niu, Z.; Gibson, H. W. *Chem. Rev.* **2009**, *109*, 6024.

(8) (a) Lee, E. Y.; Jang, S. Y.; Suh, M. P. *J. Am. Chem. Soc.* **2005**, *127*, 6374. (b) Bauer, C. A.; Timofeeva, T. V.; Settersten, T. B.; Patterson, B. D.; Liu, V. H.; Simmons, B. A.; Allendorf, M. D. *J. Am. Chem. Soc.* **2007**, *129*, 7136. (c) Allendorf, M. D.; Bauer, C. A.; Bhaktaa, R. K.; Houka, R. J. T. *Chem. Soc. Rev.* **2009**, *38*, 1330.

(9) (a) Batten, S. R.; Robson, R. *Angew. Chem., Int. Ed.* **1998**, *37*, 1460. (b) Carlucci, L.; Ciani, G.; Proserpio, D. M. *Coord. Chem. Rev.* **2003**, *246*, 247. (c) Carlucci, L.; Ciani, G.; Proserpio, D. M. *CrystEngComm* **2003**, *5*, 269. (d) Bu, X.-H.; Tong, M.-L.; Chang, H.-C.; Kitagawa, S.; Batten, S. R. *Angew. Chem., Int. Ed.* **2004**, *43*, 192. (e) Liang, K.; Zheng, H.; Song, Y.; Lappert, M. F.; Li, Y.; Xin, X.; Huang, Z.; Chen, J.; Lu, S. *Angew. Chem., Int. Ed.* **2004**, *43*, 5776.

(10) For example: (a) Wu, H.; Yang, J.; Su, Z.-M.; Batten, S. R.; Ma, J.-F. *J. Am. Chem. Soc.* **2011**, *133*, 11406. (b) Withersby, M. A.; Blake, A. J.; Champness, N. R.; Cooke, P. A.; Hubberstey, P.; Schröder, M. *J. Am. Chem. Soc.* **2000**, *122*, 4044. (c) Long, D. L.; Hill, R. J.; Blake, A. J.; Champness, N. R.; Hubberstey, P.; Wilson, C.; Schröder, M. *Chem.—Eur. J.* **2005**, *11*, 1384. (d) Wang, X.-L.; Qin, C.; Wang, E.-B.; Li, Y.-G.; Su, Z.-M.; Xu, L.; Carlucci, L. *Angew. Chem., Int. Ed.* **2005**, *44*, 5824. (e) Wang, X.-L.; Qin, C.; Wang, E.-B.; Su, Z.-M. *Chem.—Eur. J.* **2006**, *12*, 2680. (f) Lan, Y.-Q.; Wang, X.-L.; Li, S.-L.; Su, Z.-M.; Shao, K.-Z.; Wang, E.-B. *Chem. Commun.* **2007**, 4863. (g) Xiao, D.-R.; Li, Y.-G.; Wang, E.-B.; Fan, L.-L.; An, H.-Y.; Su, Z.-M.; Xu, L. *Inorg. Chem.* **2007**, *46*, 4158. (h) Qu, X.; Xu, L.; Gao, G.; Li, F.; Yang, Y. *Inorg. Chem.* **2007**, *46*, 4775. (i) Zhang, J.; Yao, Y. G.; Bu, X. *Chem. Mater.* **2007**, *19*, 5083.

(11) (a) Zhan, S.-Z.; Li, D.; Zhou, X.-P.; Zhou, X.-H. *Inorg. Chem.* **2006**, *45*, 9163. (b) Zhang, S.-S.; Zhan, S.-Z.; Li, M.; Peng, R.; Li, D. *Inorg. Chem.* **2007**, *46*, 4365. (c) Ni, W.-X.; Li, M.; Zhou, X.-P.; Li, Z.; Huang, X.-C.; Li, D. *Chem. Commun.* **2007**, 3479. (d) Ni, W.-X.; Li, M.; Zhan, S.-Z.; Hou, J.-Z.; Li, D. *Inorg. Chem.* **2009**, *48*, 1433. (e) Liu, T. F.; Lü, J.; Guo, Z.; Proserpio, D. M.; Cao, R. *Cryst. Growth Des.* **2010**, *10*, 1489. (f) Zhang, L.; Yao, Y. L.; Che, Y. X.; Zheng, J. M. *Cryst. Growth Des.* **2010**, *10*, 528.

(12) Ma, L.; Wu, C.-D.; Wanderley, M. M.; Lin, W. *Angew. Chem., Int. Ed.* **2010**, *49*, 8244.

(13) (a) Ma, S.; Eckert, J.; Forster, P. M.; Yoon, J. W.; Hwang, Y. K.; Chang, J. S.; Collier, C. D.; Parise, J. B.; Zhou, H. C. *J. Am. Chem. Soc.* **2008**, *130*, 15896. (b) Shekhah, O.; Wang, H.; Paradinas, M.; Ocal, C.; Schüpbach, B.; Terfort, A.; Zacher, D.; Fischer, R. A.; Wöll, C. *Nat. Mater.* **2009**, *8*, 481.

(14) Farha, O. K.; Mulfort, K. L.; Thorsness, A. M.; Hupp, J. T. *J. Am. Chem. Soc.* **2008**, *130*, 8598.

(15) In previous papers such as refs 9, 11, and 12, the terminology of “self-catenation”, “self-entanglement”, “self-penetration”, or “polyknotting” is usually employed to describe such systems, but only “self-catenation” is recommended by Proserpio et al. In this paper, we prefer to use the term “self-catenation” to describe these networks. (a) Carlucci, L.; Ciani, G.; Proserpio, D. M. Networks, Topology and Entanglements. In *Making Crystals by Design: Methods, Techniques and Applications*; Braga, D., Grepioni, F., Eds.; Wiley-VCH: Weinheim, Germany, 2007; Chapter 1.3, pp 58−85. (b) Proserpio, D. M. *Nat. Chem.* **2010**, *2*, 435.

(16) (a) Marsden, J. A.; Miller, J. J.; Shirtcliff, L. D.; Haley, M. M. *J. Am. Chem. Soc.* **2005**, *127*, 2464. (b) Jayasekera, B.; Brock, S. L.; Lo, A. Y. H.; Schurko, R. W.; Nazri, G.-A. *Chem.—Eur. J.* **2005**, *11*, 3762. (c) Jose, R.; Zhanpeisov, N. U.; Fukumura, H.; Baba, Y.; Ishikawa, M. *J. Am. Chem. Soc.* **2006**, *128*, 629. (d) Huber, V.; Sengupta, S.; Wüthner, F. *Chem.—Eur. J.* **2008**, *14*, 7791. (e) Leary, E.; Higgins, S. J.; van Zalinge, H.; Haiss, W.; Nichols, R. J.; Nygaard, S.; Jeppesen, J. O.; Ulstrup, J. *J. Am. Chem. Soc.* **2008**, *130*, 12204. (f) Mishra, A.; Fischer, M. K. R.; Büerle, P. *Angew. Chem., Int. Ed.* **2009**, *48*, 2474.

(17) (a) Thomas, S. W., III; Venkatesan, K.; Müller, P.; Swager, T. M. *J. Am. Chem. Soc.* **2006**, *128*, 16641. (b) Yam, V. W. W. *Acc. Chem. Res.* **2002**, *35*, 555. (c) Zhu, M.; Aikens, C. M.; Hollander, F. J.; Schatz, G. C.; Jin, R. *J. Am. Chem. Soc.* **2008**, *130*, 5883. (d) Han, F. S.; Higuchi, M.; Kurth, D. G. *J. Am. Chem. Soc.* **2008**, *130*, 2073. (e) Armaroli, N.; Accorsi, G.; Cardinali, F.; Listorti, A. *Top. Curr. Chem.* **2007**, *28*, 69.

(18) (a) Nakano, M.; Fujita, H.; Takahata, M.; Yamaguchi, K. *J. Am. Chem. Soc.* **2002**, *124*, 9648. (b) Coe, B. J.; Harris, J. A.; Brunschwig, B. S.; Asselberghs, I.; Clays, K.; Garín, J.; Orduna, J. *J. Am. Chem. Soc.* **2005**, *127*, 13399. (c) Liao, Y.; Eichinger, B. E.; Firestone, K. A.; Haller, M.; Luo, J.; Kaminsky, W.; Benedict, J. B.; Reid, P. J.; Jen, A. K-Y.; Dalton, L. R.; Robinson, B. H. *J. Am. Chem. Soc.* **2005**, *127*, 2758. (d) Coe, B. J.; Foxon, S. P.; Harper, E. C.; Helliwell, M.; Raftery, J.; Swanson, C. A.; Brunschwig, B. S.; Clays, K.; Franz, E.; Garín, J.; Orduna, J.; Horton, P. N.; Hursthouse, M. B. *J. Am. Chem. Soc.* **2010**, *132*, 1706.

(19) For example: (a) Ford, P. C.; Vogler, A. *Acc. Chem. Res.* **1993**, *26*, 220. (b) Ford, P. C. *Coord. Chem. Rev.* **1994**, *132*, 129. (c) Vitale, M.; Ford, P. C. *Coord. Chem. Rev.* **2001**, *219−221*, 3. (d) Ford, P. C.; Cariati, E.; Bourassa, J. *Chem. Rev.* **1999**, *99*, 3625. (e) Cariati, E.; Bu, X.; Ford, P. C. *Chem. Mater.* **2000**, *12*, 3385. (f) de Angelis, F.; Fantacci, S.; Sgamellotti, A.; Cariati, E.; Ugo, R.; Ford, P. C. *Inorg. Chem.* **2006**, *45*, 10576.

(20) (a) Zhan, S.-Z.; Peng, R.; Lin, S.-H.; Ng, S. W.; Li, D. *CrystEngComm* **2010**, *12*, 1385. (b) Aggarwal, V. K.; de Vicente, J.; Bonnert, R. V. *J. Org. Chem.* **2003**, *68*, 5381. (c) Zhan, S.-Z.; Li, M.; Hou, J.-Z.; Ni, J.; Li, D.; Huang, X. C. *Chem.—Eur. J.* **2008**, *14*, 8916.

(21) (a) Trofimenko, S. *Chem. Rev.* **1972**, *72*, 497. (b) Gavrilova, A. L.; Bosnich, B. *Chem. Rev.* **2004**, *104*, 349.

(22) (a) Raptis, R. G.; Fackler, J. P., Jr. *Inorg. Chem.* **1988**, *27*, 4179. (b) Dias, H. V. R.; Diyabalanage, H. V. K.; Rawashdeh-Omary, M. A.; Franzman, M. A.; Omary, M. A. *J. Am. Chem. Soc.* **2003**, *125*, 12072. (c) Dias, H. V. R.; Diyabalanage, H. V. K.; Eldabaja, M. G.; Elbjeirami, O.; Rawashdeh-Omary, M. A.; Omary, M. A. *J. Am. Chem. Soc.* **2005**, *127*, 7489. (d) Tekarli, S. M.; Cundari, T. R.; Omary, M. A. *J. Am. Chem. Soc.* **2008**, *130*, 1669. (e) Stollenz, M.; John, M.; Gehring, H.; Dechert, S.; Grosse, C.; Meyer, F. *Inorg. Chem.* **2009**, *48*, 10049. (f) Gong, F.; Wang, Q.; Chen, J.; Yang, Z.; Liu, M.; Li, S.; Yang, G.; Bai, L.; Liu, J.; Dong, Y. *Inorg. Chem.* **2010**, *49*, 1658.

(23) (a) He, J.; Yin, Y.-G.; Wu, T.; Li, D. *Chem. Commun.* **2006**, 2845. (b) Zhang, J.-X.; He, J.; Yin, Y.-G.; Hu, M.-H.; Li, D.; Huang, X. C. *Inorg. Chem.* **2008**, *47*, 3471. (c) Zhan, S.-Z.; Li, M.; Zhou, X.-P.; Wang, J.-H.; Yang, J.-R.; Li, D. *Chem. Commun* **2011**, DOI: 10.1039/C1CC14303D.

(24) (a) Peng, R.; Li, D.; Wu, T.; Zhou, X.-P.; Ng, S. W. *Inorg. Chem.* **2006**, *45*, 4035. (b) Zhou, X.-P.; Li, D.; Wu, T.; Zhang, X. *Dalton Trans.* **2006**, 2435. (c) Zhou, X.-P.; Ni, W.-X.; Zhan, S.-Z.; Ni, J.; Li, D.; Yin, Y.-G. *Inorg. Chem.* **2007**, *46*, 2345. (d) Hou, L.; Li, D.; Shi, W.-J.; Yin, Y.-G.; Ng, S. W. *Inorg. Chem.* **2005**, *44*, 7825. (e) Li, D.; Wu, T. *Inorg. Chem.* **2005**, *44*, 1175. (f) Li, D.; Shi, W.-J.; Hou, L. *Inorg. Chem.* **2005**, *44*, 3907.

(25) Peng, R.; Li, M.; Li, D. *Coord. Chem. Rev.* **2010**, *254*, 1.

(26) (a) Tronic, T. A.; deKrafft, K. E.; Lim, M. J.; Ley, A. N.; Pike, R. D. *Inorg. Chem.* **2007**, *46*, 8897. (b) Araki, H.; Tsuge, K.; Sasaki, Y.; Ishizaka, S.; Kitamura, N. *Inorg. Chem.* **2005**, *44*, 9667.

(27) (a) Pyykko, P. *Chem. Rev.* **1997**, *97*, 597. (b) Hermann, H. L.; Boche, G.; Schwerdtfeger, P. *Chem.—Eur. J.* **2001**, *7*, 5333.

(28) Sheldrick, G. M. *Acta Crystallogr.* **2008**, *A64*, 112.

(29) (a) Dolomanov, O. V.; Blake, A. J.; Champness, N. R.; Schröder, M. *J. Appl. Crystallogr.* **2003**, *36*, 1283. (b) The program packages are available at http://www.ccp14.ac.uk/ccp/web-mirrors/lcells/olex/olex_index.htm

(30) Blatov, V. A. *Multipurpose crystallochemical analysis with the program package TOPOS. IUCr CompComm Newsletter* **2006**, *7*, 4–38. *TOPOS* is available at http://www.topos.ssu.samara.ru.

(31) (a) Bondi, A. *J. Phys. Chem.* **1964**, *68*, 441. (b) Winter, M. http://www.webelements.com/

(32) In this paper, the three-letter name for 2-D and 3-D topology networks, the point and vertex symbols instead of the Schläfli and extended Schläfli symbols, are used to describe these known networks, which are recommended by Blatov et al., according to the latest views about topological nomenclature: (a) Blatov, V. A.; O'Keeffe, M.; Proserpio, D. M. *CrystEngComm* **2009**, *12*, 44. (b) O'Keeffe, M.; Peskov, M. A.; Ramsden, S. J.; Yaghi, O. M. *Acc. Chem. Res.* **2008**, *41*, 1782. (c) The Reticular Chemistry Structure Resource (RCSR) website of O'Keeffe at http://rcsr.anu.edu.au/

(33) (a) Yeung, W. F.; Gao, S.; Wong, W. T.; Lau, T. C. *New J. Chem.* **2002**, *26*, 523. (b) Blatov, V. A.; Carlucci, L.; Ciani, G.; Proserpio, D. M. *CrystEngComm* **2004**, *6*, 377.

(34) Öhrström, L.; Larsson, K. *Molecule-Based Materials: The Structural Network Approach*; Elsevier: New York, 2005.

(35) (a) Wells, A. F. *Three-dimensional Nets and Polyhedra*; Wiley-Interscience: New York, 1977. (b) Wells, A. F. *Further Studies of Threedimensional Nets*; ACA Monograph Series No. 8; American Crystallographic Association: Buffalo, NY, 1979.

(36) (a) Angelova, O.; Macicek, J.; Atanasov, M.; Petrov, G. *Inorg. Chem.* **1991**, *30*, 1643. (b) Reineke, T. M.; Eddaoudi, M.; O'Keeffe, M.; Yaghi, O. M. *Angew. Chem., Int. Ed.* **1999**, *38*, 2590. (c) Baburin, I. A.; Blatov, V. A.; Carlucci, L.; Ciani, G.; Proserpio, D. M. *Cryst. Growth Des.* **2008**, *8*, 519.

(37) (a) Blatov, V. A. *Acta Crystallogr.* **2007**, *A63*, 329. (b) Blatov, V. A.; Proserpio, D. M. *Acta Crystallogr.* **2009**, *A65*, 202.

(38) (a) Zhang, X.-M. *Coord. Chem. Rev.* **2005**, *249*, 1201. (b) Chen, X.-M.; Tong, M.-L. *Acc. Chem. Res.* **2007**, *40*, 162.

(39) (a) Yaghi, O. M.; Li, H.; O'Keeffe, M. *Mater. Res. Soc. Symp. Proc.* **1997**, *453*, 127. (b) Carlucci, L.; Ciani, G.; Macchi, P.; Proserpio, D. M. *Chem. Commun.* **1998**, 1837. (c) O'Keeffe, M.; Eddaoudi, M.; Li, H.; Reineke, T.; Yaghi, O. M. *J. Solid State Chem.* **2000**, *152*, 3.

(40) (a) Frevel, F. L. *J. Am. Chem. Soc.* **1936**, *58*, 779. (b) Wagner, E. L. *J. Chem. Phys.* **1965**, *40*, 2728.

(41) Zhang, J.-P.; Lin, Y.-Y.; Huang, X.-C.; Chen, X.-M. *J. Am. Chem. Soc.* **2004**, *125*, 5495.